AD

CONTRACT REPORT BRL-CR-564

A MODEL FOR ANALYSIS OF SECONDARY COMBUSTION IN GUN EXHAUST PLUMES

GENERAL APPLIED SCIENCE
LABORATORIES, INC.
77 RAYNOR AVENUE
RONKONKOMA, NEW YORK

FEBRUARY 1987

US ARMY BALLISTIC RESEARCH LABORATORY
ABERDEEN PROVING GROUND, MARYLAND

UNCLASSIFIED
SECURITY CLASSIFICATION OF THIS PAGE

REPORT DOCUMENTATION PAGE

Form Approved
OMB No. 0704-0188
Exp. Date: Jun 30, 1986

1a. REPORT SECURITY CLASSIFICATION UNCLASSIFIED	1b. RESTRICTIVE MARKINGS
2a. SECURITY CLASSIFICATION AUTHORITY	3. DISTRIBUTION/AVAILABILITY OF REPORT
2b. DECLASSIFICATION/DOWNGRADING SCHEDULE	
4. PERFORMING ORGANIZATION REPORT NUMBER(S) GASL TR 276	5. MONITORING ORGANIZATION REPORT NUMBER(S) BRL-CR-564
6a. NAME OF PERFORMING ORGANIZATION General Applied Science Laboratories, Inc. — 6b. OFFICE SYMBOL (If applicable)	7a. NAME OF MONITORING ORGANIZATION
6c. ADDRESS (City, State, and ZIP Code) 77 Raynor Avenue Ronkonkoma, NY 11779	7b. ADDRESS (City, State, and ZIP Code)
8a. NAME OF FUNDING/SPONSORING ORGANIZATION US Army Ballistic Research Laboratory — 8b. OFFICE SYMBOL (If applicable) SLCBR-LF-F	9. PROCUREMENT INSTRUMENT IDENTIFICATION NUMBER DAAK11-83-C-0003
8c. ADDRESS (City, State, and ZIP Code) Aberdeen Proving Ground, MD 21005-5066	10. SOURCE OF FUNDING NUMBERS

PROGRAM ELEMENT NO.	PROJECT NO.	TASK NO.	WORK UNIT ACCESSION NO.
RDT&E	162618	AH80	

11. TITLE (Include Security Classification)
A MODEL FOR ANALYSIS OF SECONDARY COMBUSTION IN GUN EXHAUST PLUMES

12. PERSONAL AUTHOR(S)
Erdos, J., Ray, R. and Joseph, S.

13a. TYPE OF REPORT	13b. TIME COVERED	14. DATE OF REPORT (Year, Month, Day)	15. PAGE COUNT
Final	FROM _____ TO _____		

16. SUPPLEMENTARY NOTATION

17. COSATI CODES			18. SUBJECT TERMS (Continue on reverse if necessary and identify by block number)
FIELD	GROUP	SUB-GROUP	
~~20~~	06		MUZZLE FLASH, AEROTHERMOCHEMISTRY,
19	04		MUZZLE BLAST, UNSTEADY TURBULENT MIXING,

19. ABSTRACT (Continue on reverse if necessary and identify by block number)

An analytical model of the unsteady turbulent mixing and chemical reaction at the propellant-air interface in a muzzle blast flowfield has been developed. Particular attention has been given to the interplay between falling pressure and entrainment of variable-temperature gases as a key element of the processes leading to secondary combustion of the propellant in the gun exhaust plume. For the sake of computational economy, the model has been restricted to the axis of symmetry, and a two-layer integral-method has been developed. Instructions for use of the computer code are presented.

20. DISTRIBUTION/AVAILABILITY OF ABSTRACT	21. ABSTRACT SECURITY CLASSIFICATION	
☐ UNCLASSIFIED/UNLIMITED ☐ SAME AS RPT. ☐ DTIC USERS		
22a. NAME OF RESPONSIBLE INDIVIDUAL EDWARD M. SCHMIDT	22b. TELEPHONE (Include Area Code) 301-278-3786	22c. OFFICE SYMBOL SLCBR-LF-F

DD FORM 1473, 84 MAR — 83 APR edition may be used until exhausted. All other editions are obsolete.

SECURITY CLASSIFICATION OF THIS PAGE
UNCLASSIFIED

TABLE OF CONTENTS

LIST OF TABLES

LIST OF FIGURES

1.0 INTRODUCTION

Muzzle blast and flash are inherent to ejection of a chemically-propelled projectile from a gun barrel. Blast is the result of release of high-pressure gases and the ensuing over-pressure of the surrounding atmosphere. Flash is the radiation from the expelled propellant gases, which is frequently augmented by afterburning of the hydrogen-rich propellent gases in the atmosphere. Blast and flash, as well as the dispersal of propellant gases and combustion products, represent environmental hazards to the gunner and other personnel or machinery in the area of the gun platform. Additionally, they are functionally undesirable in that they reveal the gun location. Consequently, considerable effort has been devoted to development of mechanical devices which are intended to suppress blast and flash or to deflect muzzle gases away from sensitive areas (e.g., aircraft engine inlets). Although blast, flash and the distribution of propellent exhaust gases are closely interrelated phenomena, muzzle devices which are successful in achieving one objective (e.g., exhaust gas diverters and recoil attenuation devices) are often counterproductive in other areas (i.e., flash suppression).

The coupling between muzzle blast and flash is evident in the amplification of blast overpressure by propellant afterburning, in the augmentation of flash by muzzle brakes (which divert the exhaust gases), and in flash suppression by conical exhaust nozzles (which focus the exhaust gases). Blast and flash therefore clearly involve an interplay between mechanical design of the gun and chemical composition of the propellant. A more thorough discussion of the phenomenology and recent experience can be found in the studies by Keller[1],[2] and Schmidt[3], as well as in the substantial body of prior work cited therein.

The present work concentrates on development of a model of muzzle flash which embodies the essential thermo-chemistry and fluid-dynamics of the process while retaining computational simplicity appropriate to exploratory studies and engineering analyses. The essential features of the phenomenon are considered to be unsteady mixing of the propellant exhaust gases with shock-heated air and concurrent chemical reaction in a flowfield dominated by an expanding blast wave. Emphasis has been placed on identification and representation of the primary physical processes rather than detailed numerical analysis or comprehensive comparative studies.

---

1 Keller, G.E., "Secondary Muzzle Flash and Blast of the British 81-mm, L16A2, Mortar" ARBRL-MR-03117, July 1981.

2 Keller, G.E., "The Effect of Propellant Composition on Secondary Muzzle Blast Overpressure" ARBRL-MR-03270, April 1983.

3 Schmidt, E.M., "Secondary Combustion in Gun Exhaust Flows" ARBRL-TR-02373, October 1981.

The basic fluid-dynamical model draws on the muzzle blast analysis of Erdos and DelGuidice[4], which describes the unsteady flowfield along the gun axis from the muzzle to the blast wave. This model assumes, however, that the propellant gases are effectively inert after expulsion from the muzzle and neglects any mixing along their interface with the atmosphere. Both these assumptions are removed in the present model. The chemical-kinetic mechanisms governing the reaction of the propellant gases with air, including the effects of potassium additives, are drawn from the work of Yousefian[5],[6]. This work pays careful attention to the complex kinetics of the afterburning reactions and the potential for flash suppression by chemical additives. However, the fluid-dynamics are modeled by steady-state mixing with constant boundary conditions, which unfortunately ignores essential transients in pressure and variations in boundary conditions on the mixing layer due to the blast wave.[1]

The present work also draws on the study of secondary combustion by Schmidt[3]. Schmidt recognizes the essentially unsteady nature of the phenomenon, but attempts to apply the unsteady conditions to empirical flash criteria without modeling the rate of mixing or of reaction. His study is also important in that it identifies the mechanism by which muzzle brakes tend to augment flash, namely by the generation of multiple shocks. The present work does not attempt to explicitly model muzzle devices, such as brakes. However it does allow the effects of such devices to be modeled through the fluid-dynamic boundary conditions placed on the mixing layer, in the same fashion as Schmidt considers their effect on the empirical flash criteria.

Finally, the evaluation of available muzzle flash codes performed by Keller[7] is pointed out since it reinforces the requirement for a model such as proposed herein.

---

4 Erdos, J. and DelGuidice P., "Calculation of Muzzle Blast Flowfields" AIAA Journal, Vol. 13, No. 8, August 1975 pp. 1048-1056.

5 Yousefian, V., "Muzzle Flash Onset" ARBRL-CR-00477, Feb. 1982.

6 Yousefian, V., "Muzzle Flash Onset: An Algebraic Criterion and Further Validation of the Muzzle Exhaust Flow Field Model" ARBRL-CR-00506, March 1983.

7 Keller, G.E., "An Evaluation of Muzzle Flash Prediction Codes" ARBRL-MR-03318, Nov. 1983.

2.0 DISCUSSION OF THE MODEL

The essential features of a muzzle exhaust flowfield are sketched in Figure (1). The propellant gases expand supersonically upon release from the gun barrel. In a vacuum, the expansion process would approach a spherical source flow with it's origin at the muzzle. The propellant gases would form, in effect, an expanding spherical "balloon". In the atmosphere, the spherical expansion is contained by a finite back-pressure exerted by the surrounding air. This boundary condition leads to the barrel shocks which terminate the near-spherical expansion and turn the propellant gases back to a near-axial flow direction. The expanding front of propellant gases still forms a "balloon" of sorts which drives a strong shock wave, i.e., a "blast wave", into the atmosphere ahead of it. The pressure field behind the blast wave causes the supersonic propellant gases to compress to a matching pressure across another strong shock, termed the "Mach disc". The subsonic flowfield between the Mach disc and the blast wave again resembles a spherical expansion, a fact that allowed Erdos and DelGuidice[4] to model this region as a one-dimensional unsteady flow with spherical symmetry.

The supersonic portion of the propellant expansion is quasi-steady; i.e., it adjusts almost instantly to the time-varying conditions at the muzzle as the propellant gases empty from the gun. The position of the Mach disc varies continuously, but upstream of the disc the flowfield resembles a steady, under-expanded rocket plume. Mixing of the propellant gases with air will occur along the lateral boundaries of the plume, and since the propellant gases are typically rich in hydrogen and carbon monoxide, some afterburning in this mixing layer may be expected. However, since the air side of the layer is essentially quiescent while the propellant gases are moving at high supersonic speeds, and since the total (stagnation) temperature of the air is much lower than that of the propellant gases, the maximum static temperature in the mixing layer can be estimated by analogy with a hypersonic cold-wall boundary layer[8]. Accordingly, the maximum static temperature will be about one-quarter the total temperature of the propellant gases, and this temperature will occur where the velocity is about one-half the propellant velocity and the gas mixture will consist of about one-half air and one-half propellant gases. The mixture ratio and temperature would therefore favor ignition, but the velocity may inhibit ignition by allowing less time at this condition than the required ignition delay time. Characteristic gas residence time in this layer will be a small fraction of the gun emptying time.

The subsonic portion of the propellant gas expansion i.e., the portion between the Mach disc and the propellant-air interface, is decidedly non-steady. Since the Mach number of the flow is low, the static temperature of the propellant gases approaches the total temperature. Furthermore, the

---

[8] Dorrance, W.H., Viscous Hypersonic Flow, McGraw Hill Book Co., New York, 1962.

velocity is low so the residence time in this layer will approach the gun emptying time. Consequently, afterburning is far more likely in the mixing layer that develops at the propellant-air interface in this region (i.e., near the gun axis) than along the boundaries of the supersonic plume.

The static temperature of the propellant gas and of the air at their interface varies in time as the pressure drops. However, the entropy of the propellant gas and of the air at any point in the flowfield defines the thermodynamic relationship between the temperature and pressure. The time variation of entropy is governed by the energy equation which in the absence of chemical reactions, heat conduction, diffusion, etc., simply states that the entropy is convected along streamlines (particle paths) except where the streamlines cross shock waves. The entropies of the two sides of the interface are therefore determined by the initial conditions at release of the propellant gas. The blast wave begins as a strong shock wave and maintains its strength as the cumulative amount of energy released by the escaping propellant gases increases. The strength of the blast wave begins to decay, however, as it acquires a spherical shape and grows in radius. The cumulative energy released by the propellant gases also begins to asymptote to a constant as the gun barrel empties, and the blast wave decay rate transitions from the power law associated with a constant rate of energy deposition to a constant total energy release (i.e., a point explosion). The net result is that the entropy of the shock-heated air is initially about a constant near the propellant-air interface and then steadily decreases with increasing distance from the interface.

The entropy of the propellant gas, on the other hand, consists of the entropy generated by the propellant combustion process in the breech-end of the gun barrel plus the increment added as the gas passes across the plume Mach disc. The entropy layer on the propellant side of the interface therefore also exhibits a spatial variation associated with the initial increase in strength of the Mach disc, but as the Mach disc later decays in strength and collapses the propellant-side entropy asymptotes to the combustion generated value. The propellant-side flowfield therefore exhibits a significant increase in entropy with increasing distance from the interface, a maximum entropy at some point, and a subsequent decrease and asymptotic approach to the entropy of the gas venting from the muzzle.

The significance of the propellant-side and air-side entropy layers is that the shock-processed air is hot as it accumulates near the interface, and remains relatively warm as the pressure drops and volume expands. However, the hot propellant gas leaving the muzzle is further heated by the Mach disc, and as the pressure drops a temperature distribution resembling the entropy layer develops, namely: warm at the interface, hotter proceeding away from the interface to a maximum temperature, and then cooling again and asymptoting to the temperature of the gas venting through an isentropic subsonic expansion to the atmosphere. Consequently, as the gases mix along the interface, the mixing layer will initially entrain relatively hot propellant gas and air. (The term "relative" is used to denote the dependence on pressure.) As more propellant

gas is entrained, its relative temperature will increase, accelerating the rate at which afterburning reactions between the air and the unburned propellant gas proceed. The relative temperature of the entrained propellant gas will reach a maximum and then slowly decay toward an asymptotic final temperature.

Reactions between the unburned propellant gas and air are initiated in the mixing layer at very high pressure, but as the pressure drops the molecular collision frequency drops in direct proportion and the speed of the chain-forming ignition reactions may not be sufficient to sustain combustion. However, the ignition-sustaining reactions will be promoted by the entrainment of increasingly hotter propellant gas, which will offset the effect of dropping pressure to some extent, since the reaction rates are typically exponentially proportional to temperature. If the ignition reactions become self-sustaining during the period of entrainment of shock heated propellant gas, flash occurs. If they have not become self-sustaining by the time the entrained propellant gas has reached it's asymptotic decay period, there will be no flash due to afterburning.

Clearly then, the occurrence of flash is critically dependent on the competing mechanisms of falling pressure and entrainment of variable temperature propellant gas which are superimposed on the mixing process. The present model has been specifically formulated to address this phenemonology.

The role of chemical additives in the propellant is simply to interfere with the ignition process by tying up the free-radicals needed to sustain combustion. The amount of additive needed will depend on the transient fluid-mechanical characteristics of the specific muzzle flowfield. The present model is also intended to provide a capability to rapidly assess the effectiveness of chemical additives.

As the preceding discussion of the phenomology should indicate, the transient characteristics of the flowfield, particularly the pressure impressed on the mixing layer and the variation in temperature (i.e., entropy) of the entrained gas, are considered essential to evaluation of the chemical processes leading to flash. These processes occur on a time scale comparable to the characteristic time for the flowfield transients and must therefore be modeled as "finite rate" processes. Unfortunately, the cost of carrying out finite-rate chemical calculations can escalate very quickly. The fluid dynamics require solution of three equations: conservation of mass, momentum and energy. Finite-rate chemistry adds one more equation for each chemical species considered, and requires evaluation of complex reaction rate expressions for every reaction in which the considered species participates. Consequently there is a strong fiscal motivation for keeping the number of spatial locations at which the species equations must be solved to a minimum. The bare minimum is, of course, one point, e.g., the interface.

A two-layer model of the mixing layer has been adopted in which the inviscid interface divides the two layers. The governing equations for conservation of mass and energy are analytically integrated from the interface

outward to the "edge" or "front" of each layer, leading to a pair of ordinary differential equations for the thermal thickness of each layer. The momentum equation is eliminated from present consideration by restricting attention to the axis of symmetry. The integral species conservation equation is automatically satisfied by assuming the thickness of the species diffusion layer is equal to the thermal thickness.

Thus, the present model only requires solution of the governing equations at the interface, plus the two equations for the thermal thickness of each layer.

A detailed description of the analytical formulation of the two-layer model is presented in the following section.

3.0 DESCRIPTION OF THE ANALYTICAL FORMULATION

Assumptions and Basic Equations

As previously depicted in Figure (1), a mixing layer develops along the interface between the propellant gas and the air. Within this mixing layer, hot propellant gas (shock-heated by the Mach disc) is brought into contact with hot oxygen (in the air which has been shock-heated by the blast wave). The mixing layer can be viewed as two sublayers: one which extends outward from the inviscid interface between the propellant gas and air and one which extends inward from it. The inviscid interface provides a convenient frame of reference for the mixing layer.

The present model is restricted to development of a planar mixing layer at the gun axis. In other words, the radius of curvature of the inviscid interface is assumed to be much larger than the thickness of the mixing layer. Furthermore, forces due to acceleration of the interface are neglected. The latter assumption is perhaps suspect at early times, but the interface location becomes virtually steady by the time secondary combustion is usually observed. The former assumption may also be questioned for later times when the mixing layer becomes very thick. Nevertheless, the present model should adequately model the phenomena of interest, and provide a basis for further modeling as needed to refine the predictive capabililty.

The inviscid interface is therefore used as the base of a two-dimensional, rectangular coordinate system: x is the distance along the interface and y is the distance normal to it.

Modeling of the diffusive processes poses a somewhat perplexing dilemma. Shadowgraphs of muzzle blast flowfields such as those taken by Schmidt and Shear[9] show highly turbulent structures in the mixing layers. However, the propellant-air interface near the gun axis is not visible. No inviscid velocity jump exists across the interface at the axis, and hence the usual mechanism for generating turbulent motion is absent at that point. The interface cannot support a pressure jump, and therefore the pressure gradients along the interface must be identical. Consequently, differences in the velocity gradients must be associated with the differences in density across the interface. Hence, velocity jumps that develop away from the axis due to the pressure gradient are expected to be relatively small. Again, there seems to be an absence of strong driving mechanisms for turbulence generation near the axis. By contrast, the inviscid velocity jumps across the lateral boundaries of the plume are large, and the observed turbulence in this area is clearly consistent with a shear-driven mechanism.

---

[9] Schmidt, E. and Shear, D. "Flowfield About the Muzzle of an M16 Rifle" BRL Report 1692, Jan., 1974. Also, AIAA Journal, Vol. 13, PP. 1088-1093, Aug., 1975.

Acceleration of an interface between fluids of differing density in the direction of the lower density fluid gives rise to the classical Rayleigh-Taylor instability of the interface. The observed broadening of the interface and turbulent mixing of driver and driven gases in a shock tube has been attributed to this mechanism[10,11,12,13]. The interface in a shock tube is proposed herein as an possible model for the muzzle flowfield interface at the axis of symmetry.

In view of the lack of a well-defined basis for modeling the diffusive mechanism for the mixing layer that develops along the interface, three models have been postulated. The first is simply a laminar viscosity, thermal conductivity and diffusivity model. The second is a heuristic thermal conductivity model based on a classical eddy viscosity-type formulation. The third is a two-equation turbulent thermal energy model developed by analogy with the K-ε model for the turbulent kinetic energy equation. In the latter two models, the effective Lewis and Prandtl numbers are assumed to be unity.

The propellant combustion products are described as a reacting mixture of chemical species, each behaving as a perfect gas (in vibrational equilibrium). Similarly, air is described as a mixture of molecular and atomic nitrogen and oxygen, and nitric oxide (also in vibrational equilibrium). Fick's law, with a single diffusion coefficient for all combinations of species, is used to describe mass diffusion.

The thin-layer approximations to the Navier-Stokes equations will be assumed to apply, i.e.:

$$\partial^2/\partial y^2 >> \partial^2/\partial x^2 \text{ and } p = p(x,t).$$

The following set of governing equations thereby obtains (expressed here in conservative form):

---

10 Richtmeyer, R. D., "Taylor Instability in Shock Acceleration of Compressible Fluids," Communications on Pure and Applied Mathematics, Vol. 13,1960, pp. 297-319.

11 Levin, M. A., "Turbulent Mixing at the Contact Surface in a Driven Shock-Wave," The Physics of Fluids, Vol. 13, No. 5, 1970, pp. 1166-1171.

12 Andronov, V. A. et al., "Turbulent Mixing at Contact Surface Accelerated by Shock-Waves," Soviet Physics-JETP, Vol. 44, 1976, pp. 424-427.

13 Houas, L., Brun, R. and Hanana, M., "Experimental Investigation of Shock-Interface Interactions," AIAA J, Vol. 24, No. 8, August 1986, pp. 1254-1255.

$$\frac{\partial \rho}{\partial t} + \frac{\partial \rho u}{\partial x} + \frac{\partial \rho v}{\partial y} = 0 \tag{1}$$

$$\frac{\partial \rho u}{\partial t} + \frac{\partial (\rho u^2 + p)}{\partial x} + \frac{\partial (\rho uv)}{\partial y} = \frac{\partial}{\partial y} \left(\mu \frac{\partial u}{\partial y}\right) \tag{2}$$

$$\frac{\partial p}{\partial y} = 0 \tag{3}$$

$$\frac{\partial \rho h}{\partial t} + \frac{\partial \rho uh}{\partial x} + \frac{\partial \rho vh}{\partial y} = \frac{\partial}{\partial y} \left(\frac{k_T}{c_p} \frac{\partial h}{\partial y}\right) + \frac{\partial p}{\partial t} \tag{4}$$

$$\frac{\partial \rho \alpha_i}{\partial t} + \frac{\partial \rho u \alpha_i}{\partial x} + \frac{\partial \rho v \alpha_i}{\partial y} = \frac{\partial}{\partial y} \left(\rho D_T \frac{\partial \alpha_i}{\partial y}\right) + \dot{w}_i \tag{5}$$

with the following equations of state:

$$p = \rho R_o T \Sigma (\alpha_i / MW_i) \tag{6}$$

$$h = \Sigma \alpha_i \, (h_i + \Delta h_i^o) \tag{7}$$

where:

$$h_i = \int_o^T C_{p_i}(T) \, dT \tag{8}$$

and:

$$C_p = \Sigma \alpha_i \, C_{p_i} \tag{9}$$

Consideration will be further restricted to the axis ($x = 0$) where $u = 0$ and $\partial/\partial x = 0$, reducing Equations (1) - (5) to:

$$\frac{\partial \rho}{\partial t} + \frac{\partial \rho v}{\partial y} = 0 \tag{10}$$

$$\frac{\partial \rho h}{\partial t} + \frac{\partial \rho v h}{\partial y} = \frac{\partial}{\partial y}\left(\frac{k_T}{C_p}\frac{\partial h}{\partial y}\right) + \frac{dp}{dt} \tag{11}$$

$$\frac{\partial \rho \alpha_i}{\partial t} + \frac{\partial \rho v \alpha_i}{\partial y} = \frac{\partial}{\partial y}\left(\rho D_T \frac{\partial \alpha i}{\partial y}\right) + \dot{w}_i \tag{12}$$

Determination of the chemical production term, $\dot{w}_i$, will employ the method developed by Pratt[14]. This, in turn, uses the thermodynamic representation individual species developed by McBride, et.al.[15] Accordingly, a fifth-order polynomial is used in the present analysis for the sensible enthalpy and specific heat of each species:

$$h_i = \sum_{j=1}^{5} C_{ij}\, T^j/_j \tag{13}$$

$$Cp_i = \sum_{j=1}^{5} C_{ij}\, T^{j-1} \tag{14}$$

The sixth coefficient defined by McBride, et.al.[15], is identified herein as the heat of formation at Δh_i^o. These coefficients are additionally used to define the equilibrium constant and either the forward or backward rate constant (whichever is not otherwise specified) from the Law of Mass Action.

Details of the technique for determination of the chemical production term $\dot{w}_i$ are provided in Reference 14. For the present discussion it may be regarded as a "source" term for Equation (12) that is a function of the instantaneous pressure, enthalpy and mixture composition:

$$\dot{w}_i = f(p, h, \alpha_j) \; ; \; j = 1, NS \text{ and } i = 1, NS \tag{15}$$

The CREK code described in Reference 14 is contained in the present computermodel as an auxiliary program that integrates Equation (15) by the Newton-Raphson iteration technique described in Reference 14:

---

[14] Pratt, D.T., "Calculation of Chemically Reacting Flows with Complex Chemistry" in Studies in Convection, B.E. Launder, Ed., Academic Press, NY 1977.

[15] McBride, B.J., Heims, S., Ehlers, J.G. and Gordon, S., "Thermodynamic Properties to 6000°K for 210 Substances", NASA SP-30001, 1966.

$$\Delta\alpha_{i_{reaction}} = \int_{t}^{t+\Delta t} \frac{w_i}{\rho}\, dt \qquad (16)$$

This integration is performed at constant pressure and enthalpy, but includes the variation in temperature, density and composition due to reactions. (The scheme admits both finite-rate reactions and fully-equilibrated reactions; only the finite-rate option is of present interest.) Blending of the change in composition due to reactions with the change due to diffusion will be discussed later in connection with the solution of Equation (12). However, it should be recognized that the changes in temperature and density obtained in this step of the solution are incomplete - the complete changes are obtained from the solution of Equation (10) and (11). The influence of reactions enters implicitly through the use of Equations (6) and (7). If, for example, Equation (11) had been written in terms of temperature rather than enthalpy, a temperature "source" term involving the product $\dot{w}_i \Delta h_i^o$ would appear and the change in temperature obtained concurrently with the solution of Equation (16) would be used to represent time-integration of this term.

Integral Form of the Continuity and Energy Equations

Equations (10) and (11) can be converted from a pair of partial differential equations in two independent variables (y and t) to a pair of ordinary differential equations with time (t) as the independent variable by analytically integrating over y and representing the integrals in terms of shape parameters that are functions of time. The limits of integration are the outer edge of the mixing layer on the propellant side, δ_2, and the outer edge of the mixing layer on the air-side, δ_1. We choose to form a pair of equations by integrating first from y = 0 to $y = \delta_1$ and again from y = 0 to $y = \delta_2$. The subscripts 0, 1 and 2 will be used hereafter to denote conditions at $y = 0$, δ_1 and δ_2 respectively.

The continuity equation, Equation (10), becomes:

$$\frac{d}{dt} \int_{o}^{\delta_i} \rho dy - \rho_i \frac{d\delta_i}{dt} + \rho_i v_i = 0 \quad (i = 1,2) \qquad (17)$$

where the boundary conditions $v = 0$ at $y = 0$ and $\partial/\partial y = 0$ at $y = \delta_i$ have been imposed and L'Hopital's rule has been observed.

The energy equation, Equation (11), similarly becomes:

$$\frac{d}{dt}\int_o^{\delta_i} \rho h dy - \rho_i h_i \frac{d\delta i}{dt} + \rho_i v_i h_i$$

$$= \frac{k_{To}}{C_{po}} \left(\frac{\partial h}{\partial y}\right)_o + \frac{d}{dt}(p\delta_i) - p\frac{d\delta_i}{dt} \qquad (18)$$

The velocity v_i can be eliminated by multiplying (17) by h_i and substituting it into (18), giving:

$$\frac{d}{dt}\int_o^{\delta_i} \rho h dy - h_i \frac{d}{dt}\int_o^{\delta_i} \rho dy = -\frac{k_{To}}{C_{po}} \frac{\partial h}{\partial y_o} + \delta \frac{dp}{idt} \quad (i = 1,2) \qquad (19)$$

Evaluation of the integrals in Equation (19) requires representation of the integrands by some appropriate distribution functions satisfying the boundary conditions at $y = \delta_1$ and δ_2. Additional accuracy can be obtained by also satisfying the differential equations ((10 and (11)) at $y = 0$. Again, continuity can be substituted into the energy equation to eliminate $(\partial v/\partial y)_o$, yielding:

$$\rho_o \frac{dh_o}{dt} = \left(\frac{\partial}{\partial y}\left(\frac{k_T}{C_p}\frac{\partial h}{\partial y}\right)\right)_o + \frac{dp}{dt} \qquad (20)$$

Distribution Functions

Let f(y) represent any of the dependent variables. The boundary conditions are:

$$\frac{\partial}{\partial y} = 0 \text{ and } f = f_i \qquad \text{at } y = \delta_i \qquad (21)$$

$$f = f_o \qquad \text{at } y = 0 \qquad (22)$$

The following Fourier series is chosen to represent f(y):

$$f = a + b\cos \pi\eta + c\cos 2\pi\eta \qquad (23)$$

where $\eta = (y - \delta_2)/(\delta_1 - \delta_2)$ (24)

This series automatically satisfies the derivative condition in (21). The coefficients a, b and c are defined by the remaining boundary conditions:

$$a = (-f_o + \tfrac{1}{2}(f_2 - f_1)\cos\pi\eta_o + \tfrac{1}{2}(f_2 + f_1)\cos 2\pi\eta_o)/(\cos 2\pi\eta_o - 1) \quad (25)$$

$$b = \tfrac{1}{2}(f_2 - f_1) \quad (26)$$

$$c = (f_o - \tfrac{1}{2}(f_2 + f_1) - (f_2 - f_1)\cos\pi\eta_o)/(\cos 2\pi\eta_o - 1) \quad (27)$$

where:

$$\eta_o = -\delta_2/(\delta_1 - \delta_2) \quad (28)$$

Note that a, b, c and η_o are functions of time only. Their time derivatives are:

$$\dot{\eta}_o = (\delta_2\dot{\delta}_1 - \delta_1\dot{\delta}_2)/(\delta_1 - \delta_2)^2 \quad (29)$$

$$\dot{a} = (-\dot{f}_o + \tfrac{1}{2}(-\cos\pi\eta_o + \cos\pi\eta_o)\dot{f}_1 + \ldots)/(\cos 2\pi\eta_o - 1) \quad (30)$$

$$\dot{b} = \tfrac{1}{2}(\dot{f}_2 - \dot{f}_1) \quad (31)$$

$$\dot{c} = (\dot{f}_o + \tfrac{1}{2}(\cos\pi\eta_o - 1)\dot{f}_1 + \ldots)/(\cos 2\pi\eta_o - 1) \quad (32)$$

It should also be noted that a, b, c are linear functions of f_0, f_1, f2, δ_1 and δ_2:

$$\dot{a} = a_1\dot{f}_0 + a_2\dot{f}_1 + a_3\dot{f}_2 + a_4\dot{\delta}_1 + a_5\dot{\delta}_2 \quad (33)$$

$$\dot{b} = b_2\dot{f}_1 + b_3\dot{f}_2 \quad (34)$$

$$\dot{c} = c_1\dot{f}_o + c_2\dot{f}_1 + c_3\dot{f}_2 + c_4\dot{\delta}_1 + c_5\dot{\delta}_2 \quad (35)$$

The primary role of the distribution function is to permit evaluation of the integral of the function, viz:

$$\int_0^{\delta_1} f dy = a\delta_i - \frac{b(\delta_1-\delta_2)}{\pi} \sin \pi\eta_o - \frac{c(\delta_1-\delta_2)}{2\pi} \sin 2\pi\eta_o \tag{36}$$

and the derivative of the integral, viz:

$$\frac{d}{dt} \int_0^{\delta_i} f dy = a\dot{\delta}_i + \delta_i\dot{a} + \ldots \tag{37}$$

Evaluation of (37) is aided by the following definitions:

$$\gamma_1 (a) = a \tag{38}$$

$$\gamma_2(a, b, c, \delta_1) = a\delta_i - \frac{b(\delta_1-\delta_2)}{\pi}\sin \pi\eta_o - \frac{c(\delta_1-\delta 2)}{2\pi}\sin 2\pi\eta_o \tag{39}$$

$$\gamma_3(a_2, a_3, \bar{\delta}) = -(\delta_1 - \delta_2)(a_2\cos\pi\eta_o + a_3\cos 2\pi\eta_o)\bar{\delta} \tag{40}$$

$$I (a, b, c) = -(b\sin\pi\eta_o - \tfrac{1}{2} c \sin 2\pi\eta_o)/\pi \tag{41}$$

where

$$\bar{\delta} = \begin{cases} -\dfrac{\delta_1}{(\delta_1 - \delta_2)^2} & i = 1 \\ +\dfrac{\delta_2}{(\delta_1 - \delta_2)^2} & i = 2 \end{cases} \tag{42}$$

Using these functions, Equation (37) becomes:

$$\frac{d}{dt} \int_0^{\delta_1} f dy = \gamma_1(a)\dot{\delta}_i + \gamma_2(\dot{a}, \dot{b}, \dot{c}, \delta_i) + I (a, b, c)(\dot{\delta}_1 - \dot{\delta}_2)$$

$$+ \gamma_3(b, c, \frac{\delta_2}{(\delta_1 - \delta_2)^2})\dot{\delta}_1 + \gamma_3(a_2, a_3, -\frac{\delta 1}{(\delta_1 - \delta_2)^2})\dot{\delta}_2 \tag{43}$$

where $\dot{a}$, $\dot{b}$, $\dot{c}$ are given by Equations (33), (34) and (35), and

$$\gamma_2(\dot{a}, \dot{b}, \dot{c}, \delta_2) = \gamma_2(a_1, b_1, c_1, \delta_i)\,\dot{f}_o + \ldots + \gamma_2(a_5, b_5, c_5, \delta_i)\dot{\delta}_2 \tag{44}$$

Accordingly, (43) can be written as:

$$\begin{aligned}\frac{d}{dt}\int_o^{\delta_i} f\,dy = {} & [\gamma_1(a)]\dot{\delta}_1 + [\gamma_2(a_1, b_1, c_1, \delta_i)]\dot{f}_o \\ & + [\gamma_2(a_2, \beta_2, c_2, \delta_i)]f_1 \\ & + [\gamma_2(a_3, b_3, c_3, \delta_i)]\dot{f}_2 \\ & + \left[I(a, b, c) + \gamma_2(a_4, b_4, c_4, \delta_i) + \lambda_3\left(b, c, \frac{\delta^2}{(\delta_1 - \delta_2)^2}\,2\right)\right]\dot{\delta}_1 \\ & + \left[-I(a, b, c) + \gamma_2(a_5, b_5, c_5, \delta_i) + \lambda_3\left(b, c, \frac{-\delta_1}{(\delta_1 - \delta_2)^2}\,2\right)\right]\dot{\delta}_2\end{aligned} \tag{45}$$

Finally, the distribution function is also used to evaluate the first and second derivatives with respect to y at y = 0:

$$\left(\frac{\partial f}{\partial y}\right)_o = \left(\frac{\partial f}{\partial \eta}\right)_o \left(\frac{\partial \eta}{\partial y}\right)_o = \frac{-\pi}{\delta_1 - \delta_2}\,(b \sin \pi\eta_o + 2\,c \sin \pi\eta_o) \tag{46}$$

$$\left(\frac{\partial^2 f}{\partial y^2}\right)_o = \frac{-\pi^2}{(\delta_1 - \delta_2)^2}\,(b \cos \pi\eta_o + 2\,c \cos \pi\eta_o) \tag{47}$$

Species Equations

The same integration steps as performed above could be applied to the species equations, Equation (12), which would yield a system of equations similar to Equation (19) but involving a separate limit of integration δ_{ij} for the two layers (i = 1,2) and each species (j = 1, NS). However, consistent

with the assumption of unit Prandtl and Lewis numbers, it may be assumed that each species will diffuse to the "edge" of the mixing layer as defined by the conduction of heat across the layer, i.e., by the thermal thickness δ_i. Equating these thicknesses makes the integral form of the species equations redundant, and it becomes necessary to solve the species equation only at the interface location y = 0. Each of the species mass fractions will be described by a distribution function f_i of the form given by Equation (23), viz:

$$f_i = a_i + b_i \cos \pi\eta + c_i \cos 2\pi\eta \qquad (i = 1, NS) \tag{48}$$

where:

$$a_i = a_i \, (\alpha_{i0}, \alpha_{i1}, \alpha_{i2}, \delta_i, \delta_2) \tag{49}$$

$$b_i = b_i \, (\alpha_{i1}, \alpha_{i2}) \tag{50}$$

$$c_i = c_i \, (\alpha_{i0}, \alpha_{i1}, \alpha_{i2}, \delta_1, \delta_2) \tag{51}$$

and the coefficients a_i, b_i, c_i have the same properties as displayed in Equations (30) - (35) and (46), (47).

The species mass fractions at the interface are determined from Equation (12) evaluated at y = 0:

$$\rho_o \frac{d\alpha_{i0}}{dt} = \left[\frac{\partial}{\partial y}\left(\rho D_T \frac{\partial \alpha_i}{\partial y}\right)\right]_o + \dot{w}_{i_o} \tag{52}$$

Final System of Energy and Species Equation

Equations (19), (20) and (52), aided by (45), (46) and (47), form a coupled linear system of first-order ordinary differential equations. The coupling occurs through the equations of state, Equation (6) and (7). In particular, the enthalpy at the interface, h_o, yields the temperature at the interface by iterative solution of (7). The coupling can be simplified, and the iteration eliminated by differentiating the equations of state and using the density, rather than enthalpy, as the dependent variable for the energy equation:

$$\dot{P}/p = \dot{\rho}/\rho + \dot{T}/T + \overline{MW} \left(\sum_i (\dot{\alpha}_i/MW_i)\right) \tag{53}$$

and

$$\dot{h} = \sum_i \dot{\alpha}_i(h_i + \Delta h_i^o) + \sum_i \alpha_i\left(\sum_j C_{ij}T^{j-1}\right)\dot{T} \tag{54}$$

where

$$\overline{MW} = \left[\sum_i \alpha_i/MW_i)\right]^{-1} \tag{55}$$

Combining (20), (53) and (54) yields:

$$\bar{C}\dot{\rho}_o = \left[\left(\frac{k_T}{C_p}\frac{\partial^2 h}{\partial y^2}\right)_o + (a - \rho_o\bar{C})\,\dot{p} - \sum_i \dot{\alpha}_i\,\bar{D}_i\right] \tag{56}$$

where:

$$\bar{C} = -\sum_i\sum_j \alpha_i C_{ij}T^j \tag{57}$$

$$\bar{D}_i = \Delta h_i^o + \sum_j C_{ij}T^j/j \tag{58}$$

Equation (56) now replaces (20), and the system (19), (52) and (56) can be expressed in matrix form as:

$$A_{i1}\dot{\delta}_1 + A_{i2}\dot{\delta}_2 + A_{i3}\dot{\rho}_o + A_{i,3+j}\dot{\alpha}_j = B_i \tag{59}$$

where:

$$i = 1, NS + 3 \quad \text{(number of equations)} \tag{60}$$

$$j = 1, NS \quad \text{(number of species)} \tag{61}$$

$$A_{1,1} = 0 \tag{62}$$

$$A_{1,2} = 0 \tag{63}$$

$$A_{1,3} = \bar{C} \tag{64}$$

$$A_{1,3+j} = \rho_o \left[\sum \Delta h_i^o + \sum \left(1 - \frac{\overline{MW}}{MW_i} \right) C_{ij} T^j \right] \tag{65}$$

$$B_1 = \left(\frac{k_T}{c_p} \frac{\partial^2 h}{\partial y^2} \right)_o + (1 - \rho_o A_{1,3}) \dot{P} - \sum_i \dot{\alpha}_i \bar{D}_i \tag{66}$$

$$A_{2,1} = \lambda_1(a_1) + I(a_1, a_2, a_3) + \lambda_2(a_1^4, a_2^4, a_3^4, \delta_1) + \lambda_3(a_2, a_3, \delta_2/(\delta_1 - \delta_2)^2) + \ldots \tag{67}$$

$$A_{2,2} = -I(a_1, a_2, a_3) + \lambda_2(a_1^5, a_2^5, a_3^5, \delta_1) + \lambda_3(a_2, a_3, -\delta_1/(\delta_1 - \delta_2)^2) \tag{68}$$

$$A_{2,3} = \lambda_2(a_1^1, a_2^1, a_3^1, \delta_1)(h_o + A_{1,3}) + \ldots \tag{69}$$

$$A_{2,3+j} = \left(\sum_i \left(1 - \frac{\overline{MW}}{MW_i} \alpha_i \right) C_{ij} T^j \right) \lambda_2(a_1^1, a_2^1, a_{31}, \delta_1) - h_1 \lambda_2(a^1, b^1, c^1, \delta_1) \tag{70}$$

$$B_2 = \lambda_2(a_1^1, a_2^1, a_{31}, \delta_1)\left(\frac{\rho_o}{p}A_{1,3} + \delta_1\right)\dot{p} \tag{71}$$

$$-\left(\frac{k_T}{cp}\frac{\partial h}{\partial y}\right)_o - \rho_1 h_1 \lambda_2(a_1^2, a_2^2, a_3^2, \delta_1)\ldots$$

$$-\dot{\rho}_2 h_2 \lambda_2(a_1^3, a_2^3, a_3^3, \delta_1)$$

$$A_{3,1} = I(a_1, a_2, a_3) + \lambda_2(a_1^4, a_2^4, a_3^4, \delta_2) + \ldots \tag{72}$$

$$A_{2,1} = \lambda_1(a_1) - I(a_1, a_2, a_3) + \lambda_2(a_1^5, a_2^5, a_3^5, \delta_2) + \ldots \tag{73}$$

$$A_{3,3} = \lambda_2(a_1^1, a_2^1, a_3^1, \delta_2)(h_o + A_{1,3}) + \ldots \tag{74}$$

$$A_{3,3+j} = \left(\sum_i\left(1 - \frac{\overline{MW}}{MW_i}\alpha_i\right) C_{ij}T^j\right)\lambda_2(a_1^1, a_2^1, a_{31}, \delta_2) - h_2\lambda_2(a^1, b^1, c^1, \delta_2) \tag{75}$$

$$B_3 = \lambda_2(a_1^1, a_2^1, a_{31}, \delta_2)\left(\frac{\rho_o}{p}A_{1,3} + \delta_2\right)\dot{p} \tag{76}$$

$$-\left(\frac{k_T}{cp}\frac{\partial h}{\partial y}\right)_o - (\dot{\rho}h)_1\lambda_2(a_1^2, a_2^2, a_3^2, \delta_2)\ldots$$

$$-(\dot{\rho}h)_2\lambda_2(a_1^3, a_2^3, a_3^3, \delta_2)\ldots$$

and:

$$A_{3+j,1} = 0 \tag{77}$$

$$A_{3+J,2} = 0 \tag{78}$$

$$A_{3+J,3} = 0 \tag{79}$$

$$A_3{}^+{}_{j,,3+m} = \delta_{jm} \qquad \text{(Kronecker delta)} \tag{80}$$

$$B_{3+j} = \frac{1}{\rho_o} \left[\left(\frac{k_T}{cp} \frac{\partial^2 \alpha_j}{\partial y^2} \right)_o + \dot{w}_j \right] \tag{81}$$

where j = 1, NS and m = 1,NS.

In view of the fact that $A_{3+j,\ 3+m} = \delta_{jm}$ (i.e., 0 for $j \neq m$ and 1 for $j = m$) it is evident that the species equations are uncoupled and can be integrated independently of the remainder of the system (over a single time step):

$$\dot{\alpha}_i = B_{3+i} \tag{82}$$

In this case the B_i's can be redefined as:

$$B'_i = B_i - \Sigma\ A_{i,3+j}\ \dot{\alpha}_j \qquad i = 1,2,3 \tag{83}$$

Furthermore, since $A_{11} = A_{12} = 0$:

$$\dot{\rho}_o = B'_1 / A_{1,3} \tag{84}$$

The B'_2 and B'_3 can be redefined again as:

$$B''_2 = B'_2 - A_{2,3}\dot{\rho}_o \tag{85}$$

$$B''_3 = B'_3 - A_{3,3}\dot{\rho}_o \tag{86}$$

and the remaining 2 by 2 system is:

$$A_{2,1}\ \dot{\delta}_1 + A_{2,2}\dot{\delta}_2 = B''_2 \tag{87}$$

$$A_{3,1}\ \dot{\delta}_1 + A_{3,2}\dot{\delta}_2 = B''_3 \tag{88}$$

which is easily solved:

$$\dot{\delta}_1 = \frac{B''_2 A_{3,2} - B''_3 A_{2,2}}{A_{2,1} A_{3,2} - A_{3,1} A_{2,2}} \tag{89}$$

$$\dot{\delta}_2 = \frac{B''_3 A_{2,1} - B''_2 A_{3,1}}{A_{2,1} A_{3,2} - A_{3,1} A_{2,2}} \tag{90}$$

Thus the final system of differential equations consists of (81), (83), (87) and (88). These are integrated over a time step by a standard Runge-Kutta procedure.

Turbulence Modeling

Three options are provided in the computer code for representation of the thermal conductivity k_T and species diffusivity D_T. It should be noted that k_T only appears in ratio to C_p and D_T only appears in a product with ρ. Hence, for unit Prandtl and Lewis numbers:

$$k_T/C_p = \rho D_T = \mu \tag{91}$$

The first option is to use the laminar viscosity provided by Sutherland's law:

$$\mu = S_1 \, T^{3/2} / (T + S_2) \tag{92}$$

where S_1 and S_2 are constants in the appropriate set of units (e.g., $S_1 = 2.27 \times 10^{-8}$ lb sec/ft^2/°R$^{\frac{1}{2}}$ and $S_2 = 198.6$°R).

The second option is to use a modified form of eddy viscosity; the following is proposed here (based on analogy with accepted kinematic models):

$$\mu = S_3 \left(\sqrt{h_1} \, \delta_1 \, (\rho_1 - \rho_0) + \sqrt{h_2} \, \delta_2 \, (\rho_2 - \rho_0) \right) \tag{93}$$

where S_3 is an empirical constant. (We have used $S_3 = .0143$ lb sec/ft^2 in the code.)

The third option is to use a model of the two-equation turbulent thermal energy equation. The model is derived by analogy with the widely-used two-equation model of the turbulent kinetic energy equation. The two variables in the present model are the mean square temperature fluctuation $\overline{\theta^2}$ and a thermal dissipation coefficient, ϕ. The thermal conductivity is related to these variables by:

$$k_T = C_o \rho C_p \overline{\theta^2}/\phi \tag{94}$$

These two variables are governed by differential equations developed from the turbulent thermal energy equation by analogy with the model equations for the turbulent kinetic energy equation:

$$\rho \frac{D\overline{\theta^2}}{Dt} - \frac{k_T}{C_p}\left(\frac{\partial T}{\partial y}\right)^2 - \frac{\partial}{\partial y}\left(\frac{k_T}{C_p}\frac{\partial \overline{\theta^2}}{\partial y}\right) + \rho\phi = 0 \tag{95}$$

$$\rho \frac{D\phi}{Dt} - C_1 \frac{k_T}{C_p}\frac{\phi}{\overline{\theta^2}}\frac{\partial T}{\partial y}^2 - C_2 \frac{\partial}{\partial y}\left(\frac{k_T}{C_p}\frac{\partial \phi}{\partial y}\right) + C_3 \rho \frac{\phi^2}{\theta^2} + 0 \tag{96}$$

We have assumed that both $\overline{\theta^2}$ and ϕ can be described by the same distribution function used for the other variables, Equation (23),which, however, implies that their ratio is independent of y, and hence k_T/Cp and ρD_T are likewise independent of y. It is therefore only necessary to evaluate Equation (93) and (94) at the interface, y = 0, to obtain the differential equations for $\overline{\theta_o}^2$ and ϕ_0:

$$p_o \overline{\theta_o^2} = \frac{k_T}{C_p}\left(\left(\frac{\partial T}{\partial y}\right)^2 + \frac{\partial^2 \overline{\theta^2}}{\partial y^2}\right)_o - \rho_o \phi_o = 0 \tag{97}$$

$$\rho_o \dot{\phi} = \frac{k_T}{C_p}\left(C_1 \frac{\phi_o}{\theta_o^2}\left(\frac{\partial T}{\partial y}\right)^2 + C_2 \frac{\partial^2 \phi}{dy^2}\right)_o - C_3 \rho_o \frac{\phi_o^2}{\theta_o^2} = 0 \tag{98}$$

In this case, Equations (95) and (96) are added to the system of equations to be integrated, and $\overline{\theta}_o^2$ and ϕ_0 are added to the list of dependent variables.

Chemical Kinetics Modeling

The final form of the species equation,Equation (82), can be written as:

$$\dot{\alpha}_i = \dot{\alpha}_{i\,\text{diffusion}} + \dot{\alpha}_{i\,\text{reaction}} \qquad (99)$$

where $\dot{\alpha}_{i\,\text{diffusion}}$ and $\dot{\alpha}_{i\,\text{reaction}}$ are identifiable with the two terms in B_{3+i}, Equation (81). Equation (97) can be integrated in a variety of ways, offering various advantages in speed, simplicity, stability, etc. We have found the most stable procedure to be to evaluate $\dot{\alpha}_{i\,\text{reaction}}$ first, by calling the CREK code to integrate the chemical production rate over the time step Δt. Equation (82) is then integrated by the same Runge-Kutta scheme as the continuity and energy equations, yielding the combined effects of diffusion and reaction. The permissible step size Δt is governed by an error bound applied to all equations integrated by the Runge-Kutta procedure. However, when the rate of chemical reaction becomes very fast, the integration procedure in CREK can be stable but yield changes in composition that are too large for the Runge-Kutta procedure to integrate accurately. Therefore, no more than a 180°R change in temperature due to reaction is permitted in any time step. If this limit is exceeded the time step is halved and the evaluation of $\alpha_{i\,\text{reaction}}$ is repeated before proceeding to the Runge-Kutta integration.

The CREK code is very versatile, as well as accurate and stable. The chemical constituents of the mixture are specified by their chemical names, the polynomial coefficients defining their enthalpy, C_{ij}, and the atomic weights of the elements making up the constituents. The kinetic rate mechanism is defined symbolically by the names of the reactants and products in each reaction and either the forward or backward rate constant in the form

$$k_i = 10^{A_i} T^{B_i} \exp\left(-C_{i/T}\right) \qquad (100)$$

All this data is specified in an input file and is therefore easily modified (without any recoding).

4.0 DESCRIPTION OF THE COMPUTER CODE

Overview

The preceding analysis, while complicated in derivation, results in a fairly compact and efficient computer code. The Fortran code UMLAC (Unsteady Mixing Layer and Chemistry) executes on an HP 1000 minicomputer using the EMA (Extended Memory Area) capability of this machine. Although the calls to the CREK program are inefficient (the main program transfers data to CREK, then suspends itself while CREK executes, (including a complete initialization of the thermodynamic and kinetic rate data for each call,) CREK passes its results back to the main program, which then resumes execution,) the running times are not unreasonable (i.e., 10's of minutes, typically.) A modest amount of recoding to include the CREK code as a true set of sub-routines and eliminate the reinitialization would substantially accelerate the execution speed.

Input data is contained on three formatted ASCII files; one is read by the main program on logical unit 5, the second is read by the main program on logical unit 9, and the third is read by both the main program and by CREK on logical unit 15. The first file contains the initial conditions and integration parameters for the case at hand. The second contains the boundary condition data, i.e., pressure, inviscid flow densities on the air-side and propellant-side of the interface, and species mass fractions on both sides, all as functions of time. The third contains the thermodynamic and kinetic rate data; the thermodynamic data is read by both UMLAC and CREK.

In view of the importance of the inviscid entropy layer on the propellant-side of the interface pointed out in the earlier discussion, the program permits up to 11 streamlines in the propellant-side flowfield to be specified as part of the boundary condition data. The local "edge" properties are obtained by linear interpolation in the y direction using the value of δ_2 at the current time step, as indicated in Figure (2). Since the task of preparing this massive amount of boundary data is quite formidable, a pre-processor code DCREK has been written to provide an automated link between the inviscid muzzle blast flowfield code DAWNA[16] and the present mixing layer code UMLAC. DCREK reads the pressure history along the interface from DAWNA and the densities along each of the selected streamlines. (The density is isentropically adjusted to the interface pressure should a pressure difference exist between the streamline and the interface). It also reads the initial chemical composition for the streamlines, which can be equated to the equilibrium composition of the propellant gases at the muzzle exit, since that composition remains effectively frozen through the subsequent supersonic expansion and

---

16 Ranlet, J. and Erdos, J. "Description of Fortran Program DAWNA for Analysis of Muzzle Blast Flowfield" BRLCR-302, March 1975.

recompression across the Mach disc. DCREK converts the pressure and density to an enthalpy history for each streamline using the initial composition, and then performs a finite-rate calculation along the streamline (preserving the pressure-enthalpy history). DCREK stores the pressure, composition and (post-reaction) density history for each streamline on an output file that becomes the input data file for UMLAC. The same calculation is also performed on the air-side, but only for the interface streamline. DCREK automatically initializes the air-side composition to a mixture of 76.55% N_2 and 23.45% O_2 (by mass).

Since the same thermodynamic and kinetic-rate data file is used by CREK in both the DCREK and UMLAC codes, it should include the appropriate air constituents and air reaction mechanisms as well as the propellant gas constituents and mechanisms. For typical muzzle blast conditions the air constituents are N_2, N, O_2, O and NO, and the reactions among them are oxygen dissociation and the Zeldovich mechanism for nitric oxide formation:

$$O_2 + M \rightleftarrows O + O + M \qquad (101)$$

$$N_2 + O \rightleftarrows NO + N \qquad (102)$$

$$O_2 + N \rightleftarrows NO + O \qquad (103)$$

Input data

The initial conditions and option control data for UMLAC are given in 4 + NS number of lines, where NS is the number of species. The format and variables are shown in Table 1, and the variables are defined as follows:

Line 1:	CI	Initial value of time step, Δt
	ER	Max integration error in any variable per time step
	FCT	Initial value ratio $\delta_1/(\delta_1 + \delta_2)$
Line 2:	TINT	Initial value of time
	DELINT	Initial value of total thickness, $\delta_1 + \delta_2$
	TFINAL	Final time (at which run is terminated)
	DINF	Reference length (e.g., gun barrel diameter)
	THETIN	Initial value of $\overline{\theta_o^2}$ (if used)
	DHINT	Initial value of φ (if used)
Line 3:	KINT	Initial value of time step-counter (e.g., 0)

	KFINAL	Maximum value of time step counter
	LINT	Print interval counter
	ITURB	Turbulence model flag: -1 for the two-equation TTE model, 0 for the eddy viscosity (conductivity) model, +1 for laminar viscosity (Sutherland's law)
	ICHEM	Chemistry flag: 0 for frozen flow, 1 for finite-rate kinetics, 2 for fully equilibrated chemistry.
	IWRITE	Debug flag: 0 for normal printout, 1 for comprehensive data dumps
Line 4:	IALP	Number of species, NS
	IELE	Number of elements
Lines 4 + NS:		
	MW(I)	Molecular weight of i^{th} species
	RNAME(I)	Chemical name of i^{th} species
	DUM	Dummy variable; not used

In addition, certain semi-permanent data is stored in DATA Statements contained in a BLOCK DATA subroutine. The variables and their currently assigned values are:

CO, C1, C2, C3	=	0.09, 1.43, 0.77, 1.92
PINF	=	2117. psf
RHOINF	=	0.002376 slugs/ft^3
GAMINF	=	1.4
CPINF	=	6006. $ft^2/sec^2/°R$

The nondimensional constants are the values of C_0, C_1, C_2 and C_3 appearing in the two-equation TTE turbulence model. The values of pressure,density, ratio of specific heats and specific heat at constant pressure correspond to standard atmospheric conditions. Certain variables transferred into UMLAC from DCREK may be non-dimensionalized with respect to these parameters, as well as the reference length DINF appearing in Line 2 of the input data file. The values of these parameters in entirely arbitrary, and they may be all defined as 1.0, for example, or may be defined in S.I units, etc. The only important consideration relative to their definition is that they are assigned consistent values in DCREK and UMLAC. (In this respect, values of 1.0 may be the best choice.)

The boundary conditions are given on a second input file, as described in Table 2. In general, this file will be automatically generated by Program DCREK and require no alterations by the user. However, it can be manually prepared, if desired. The variables are defined as follows:

Line 1:	IALP	Number of Species, NS
	NSL	Number of streamlines on side #2 (max of 11)
	ISCT(1)	Number of dummy entries in the data for the i^{th} streamline (corresponds to the time it takes before the i^{th} streamline crosses the Mach disc).
Line 2:	TFIT	Time (at which the following values occur)
	P	Pressure
	RHO2(1)	Density on side #2 of the interface
	RHO1	Density on side #1 of the interface
	RHO2(I)	Density on i^{th} streamline on side #2 (I=2, NSL)
Line 3:	ALPHA2(1,I)	Mass fractions of species #1 through NS on side #2 of the interface.
Line 4:	ALPHA1(I)	Mass fractions on side #1 of the interface.
Line 5:	ALPHA2(J,I)	Mass fractions on j^{th} streamline on side #2.

*** The order of the species must match that used in lines 5 through 4 + NS on the input data file on logical unit 5 (Table 1) and that used in the THERMO section of the CREK data file (Table 3). ***

Line 6:	ZSL(J)	Axial distance from interface to the j^{th} streamline.

The thermodynamic and reaction kinetic data is on a third input file, which is described in Table 3. This file is read by the Program CREK which is called by UMLAC, and the identical file should be used by DCREK to generate the boundary condition data. The variables in this file are defined as follows:

Line 1:	ELEMENTS	Key word identifying the type of data which follows
Line 2:	NAME (I)	Chemical name of the i^{th} element
	ATWT(I)	Atomic weight of the i^{th} element
	VAL (I)	Valence of the i^{th} element
Line 3:	THERMO	Key word identifying the type of data which follows

Line 4:	NAME (I)	Chemical name of i^{th} species
	T1(I)	Upper limit of temperature range for first set of polynomial coefficients
	T2(I)	Upper limit of temperature range for second set of polynomial coefficients
Line 5:	C(I,J)	7 polynomial coefficients, as defined by Reference (10), for the first temperature range, followed by 7 more for the second temperature range.
Line 6:	MECHANISM	Key work identifying type of data which follows
Line 7:	D,E,F,G,H,I	Chemical names of reactants and products. M denotes a third-body which can be any species.
	A,B,C	Terms in the rate constant given by $k=10^{A}T^{B}$ exp (-C/T)
	K	K can be either a blank or one of the following 4 character expressions: REVE denotes that reverse rate data has been specified, CGS denotes that the data is not in S.I. units, COMM denotes a comment line (not interpreted as data). Any other expression will be ignored.

Sample data sets for the input data, boundary condition data, and thermo and kinetic data files are presented in Figures (3), (4) and (5).

Output Data

The output from UMLAC is divided into three categories. The first is a repetition of input data (in card image format) to assist in checking for input errors. The record is a set of statements of calculated constants and initial conditions. The third, which comprises most of the output, is a statement of the solution and boundary conditions. A sample output is provided in Figure 6.

The first block of data is the repetition of the data read from LU # 5, and matches the description given in Table 1. The initial part of the output data shown in Figure 6 matches the input data shown in Figure 3.

Following this is a short summary of calculated scale factors used to nondimensionalize certain variables in the program, and a message indicating that the data file on LU # 9 (Figure 4) has been successfully read. Thereafter is a synopsis of the streamline data showing the initial time and postion at which each streamline begins. The warning statement at the end of this set of data cautions the user that if the program continues beyond 0.02898 seconds it will use the boundary data at that time to the final time, 0.10 seconds in this example.

The set of calculated initial conditions for the species are given next, in the same format as used previously for the species input data on LU # 5. In this instance the first two columns of data now contain the mass fractions of the species on the air side of the interface (i.e. at $y = \delta_1$) and on the propellant side (i.e. at $y = \delta_2$). The latter values have been interpolated from the streamline data at the initial time.

The solution data begins with a set of labels identifying the current value of the time set counter, K. The following glossary identifies the output variables in the order they appear :

K	Time step counter
TIME	Current time (seconds)
DELTA 1	Thickness of air-side layer; δ_1 (ft)
DELTA 2	Thickness of propellant-side layer; δ_2 (ft)
THETA ** 2	Mean-squared temperature fluctuation; $\overline{\theta_o^2}$
PHI	Thermal energy dissipation parameter; ϕ
RHO	Density at $y = 0$; ρ_o (non dimensional)
KTO	Thermal conductivity at $y = 0$
P	Pressure (non dimensional)
RH1	Density at $y = \delta_1$; ρ_1
RH2	Density at $y = \delta_2$; ρ_2
TEMP1	Temperature at $y = \delta_1$, T_1 (°R)
TEMP2	Temperature at $y = \delta_2$, T_2 (°R)
YZERO	Location of δ_2 in streamline coordinate system
TEMP	Temperature at $y = 0$, T_o (°R)
H	Enthalpy at $y = 0$, h_o (ft^2/sec^2)
ALPHA	Array of species mass fractions at $y = 0$; α_{i_o} (same order as given by the user in the input data files.)
DPDT	dp/dt

DRH1DT	$(d\rho h/dt)$ at $y = \phi_1$
DRH2DT	$(d\rho h/dt)$ at $y = \phi_2$
ALPHA1	Mass fractions at $y = \delta_1$; α_{i_1}
DALP1DT	$(d\alpha_i/dt)$ at $y = \delta_1$
ALPHA2	Mass fractions at $y = \delta_2$; αi_2
DALP2DT	$(d\alpha_i/dt)$ at $y = \delta_2$

Following each solution statement is a set of 3 integer numbers that relate to the integration algorithm. The normal values are 4, 1 and 1. Also shown here are the current values of the (nondimensional) time step and the values that will be attempted on the next step.

The solution data will be repeated until either K > KFINAL or TIME > TFINAL.

The presence of muzzle flash is characterized by the occurrence of a rapid increase in the interface temperature (TEMP), which otherwise drops off as the pressure (P) decays and tends to remain bracketed by the bounding temperatures (TEMP1 and TEMP2). The species composition at the interface (ALPHA) provides additional diagnostic information regarding the chemical reactions leading to or suppressing flash. In general, the user is advised to examine the time variations of pressure (P) and temperature (TEMP) to determine if flash occurs in a particular case, and then examine the time histories of the species (ALPHA), the thicknesses of the two layers (DELTA1 and DELTA2), and the bounding temperatures (TEMP1 and TEMP2) for diagnostic information.

5.0 SUMMARY

A model of one-dimensional, unsteady turbulent mixing and chemical reaction along the interface between the propellant gas expelled from a gun muzzle and the blast-heated air has been developed. The model incorporates all the essential aspects of the unsteady flowfield processes, but the computational burden is economized considerably by employing a two-layer integral-method for solving the governing gas-dynamic equations. Derivation of the integral-method of analysis and of the resulting system of coupled, first order ordinary differential equations has been presented in detail. Assumption of unit Lewis and Prandtl numbers and of a single definition of the "edge" of the mixing layer for enthalpy and for species diffusion nearly uncouples the energy equation from the species conservation equation, and requires that the species equation be solved only at the interface (at no small savings in computer time).

The general requirements for operating the computer code and the specific input and output data formats and a glossary of Fortran variables have been presented.

TABLE 1

DATA FORMAT FOR UMLAC INPUT FILE
(Read on Logical Unit 5)

Line	Format	Variables
1	3E 10.	CI, ER, FCT
2	6E10.	TINT, DELINT, TFINAL, DINF, THETIN, DHINT
3	615	KINT, KFINAL, LINT, ITURB, ICHEM, IWRITE
4	215	IALP, IELE
5	3E10.,A4, 5X,A4	DUM, DUM, MW(1), DUM, RNAME (1)
6	"	" " " " "
.		
.		
.		
4 + IALP	"	" " " " "

TABLE 2

DATA FORMAT FOR UMLAC BOUNDARY CONDITION FILE
(Read on Logical Unit 9)

Line	Format	Variables
1	1215	IALP, NSL, (ISCT(I), I=2, NSL)
*** 1 + (IALP-1)/6 lines are skipped ***		
2	6E12	TFIT, P, RHO2(1), RHO1, (RHO2(I), 1=2, NSL)
3	6E12	(ALPHA2(1,I), I = IALP)
4	6E12	ALPHA1(I), I=1, IALP
5	6E12	(ALPHA2(J,I), I=1,IALP)
*** Line 5 is repeated for J=2, NSL ***		
6	6E12	(ZSL(I), I=1,NSL)

*** Lines 2 through 6 are repeated up to 91 times. The READ loop will terminate upon encountering an end-of-file mark. ***

TABLE 3

DATA FORMAT FOR CREK INPUT FILE
(Read on logical unit 15)

Line	Format	Variables
1	12A4	ELEMENTS, a key name
2	A2, 7X, 2F10	NAME (I), ATWT(I), VAL(I)

*** Line 2 is repeated for each element in the chemical system. A blank line signals the end of the elemental data ***

3	12A4	THERMO. a key name
4	A12, 27X, 2F10	NAME (I), T1(I), T2(I)
5	5E15	(C_1 (I,J), J=1,5)
6	5E15	(C_1 (I,J), J=6,7) (C_2(I,J), J=1,3)
7	5E15	(C_2 (I,J), J=4,7)

*** Lines 4-7 are repeated for each species in the chemical system. A blank line signals the end of the chemical data. Note that the number, names and order of the species must agree with the data specified in other input files. ***

8	12A4	MECHANISM, a key name
9	12A4, 3F8.3, 2A4	D,E,F,G,H,I,A,B,C,K

*** Line 9 is repeated for each reaction. It can be used to specify either the forward or backward rate of a reaction, in which case the opposite rate is calculated from the equilibrium constant, or it can be used to specify both forward and backward rates (2 lines per reaction). A blank line signals the end of the kinetics data. ***

REFERENCES

1. Keller, G.E., "Secondary Muzzle Flash and Blast of the British 81-mm, L16A2, Mortar" ARBRL-MR-03117, July 1981.

2. Keller, G.E., "The Effect of Propellant Composition on Secondary Muzzle Blast Overpressure" ARBRL-MR-03270, April 1983.

3. Schmidt, E.M., "Secondary Combustion in Gun Exhaust Flows" ARBRL-TR-02373, October 1981.

4. Erdos, J. and DelGuidice P., "Calculation of Muzzle Blast Flowfields" AIAA Journal, Vol. 13, No. 8, August 1975 pp. 1048-1056.

5. Yousefian, V., "Muzzle Flash Onset" ARBRL-CR-00477, Feb. 1982.

6. Yousefian, V., "Muzzle Flash Onset: An Algebraic Criterion and Further Validation of the Muzzle Exhaust Flow Field Model" ARBRL-CR-00506, March 1983.

7. Keller, G.E., "An Evaluation of Muzzle Flash Prediction Codes" ARBRL-MR-03318, Nov. 1983.

8. Dorrance, W.H., Viscous Hypersonic Flow, McGraw Hill Book Co., New York, 1982.

9. Schmidt, E. and Shear, D. "Flowfield About the Muzzle of an M16 Rifle" BRL Report 1692, Jan., 1974. Also, AIAA Journal, Vol. 13, PP. 1088-1093, Aug., 1975.

10. Richtmeyer, R. D., "Taylor Instability in Shock Acceleration of Compressible Fluids," Communications on Pure and Applied Mathematics, Vol. 13,1960, pp. 297-319.

11. Levin, M. A., "Turbulent Mixing at the Contact Surface in a Driven Shock-Wave," The Physics of Fluids, Vol. 13, No. 5, 1970, pp. 1166-1171.

12. Andronov, V. A. et al., "Turbulent Mixing at Contact Surface Accelerated by Shock-Waves," Soviet Physics-JETP, Vol. 44, 1976, pp. 424-427.

13. Houas, L., Brun, R. and Hanana, M., "Experimental Investigation of Shock-Interface Interactions," AIAA J, Vol. 24, No. 8, August 1986, pp. 1254-1255.

14. Pratt, D.T., "Calculation of Chemically Reacting Flows with Complex Chemistry" in Studies in Convection, B.E. Launder, Ed., Academic Press, NY 1977.

15. McBride, B.J., Heims, S., Ehlers, J.G. and Gordon, S., "Thermodynamic Properties to 6000°K for 210 Substances", NASA SP-30001, 1966.

16. Ranlet, J. and Erdos, J. "Description of Fortran Program DAWNA for Analysis of Muzzle Blast Flowfield" BRLCR-302, March 1975.

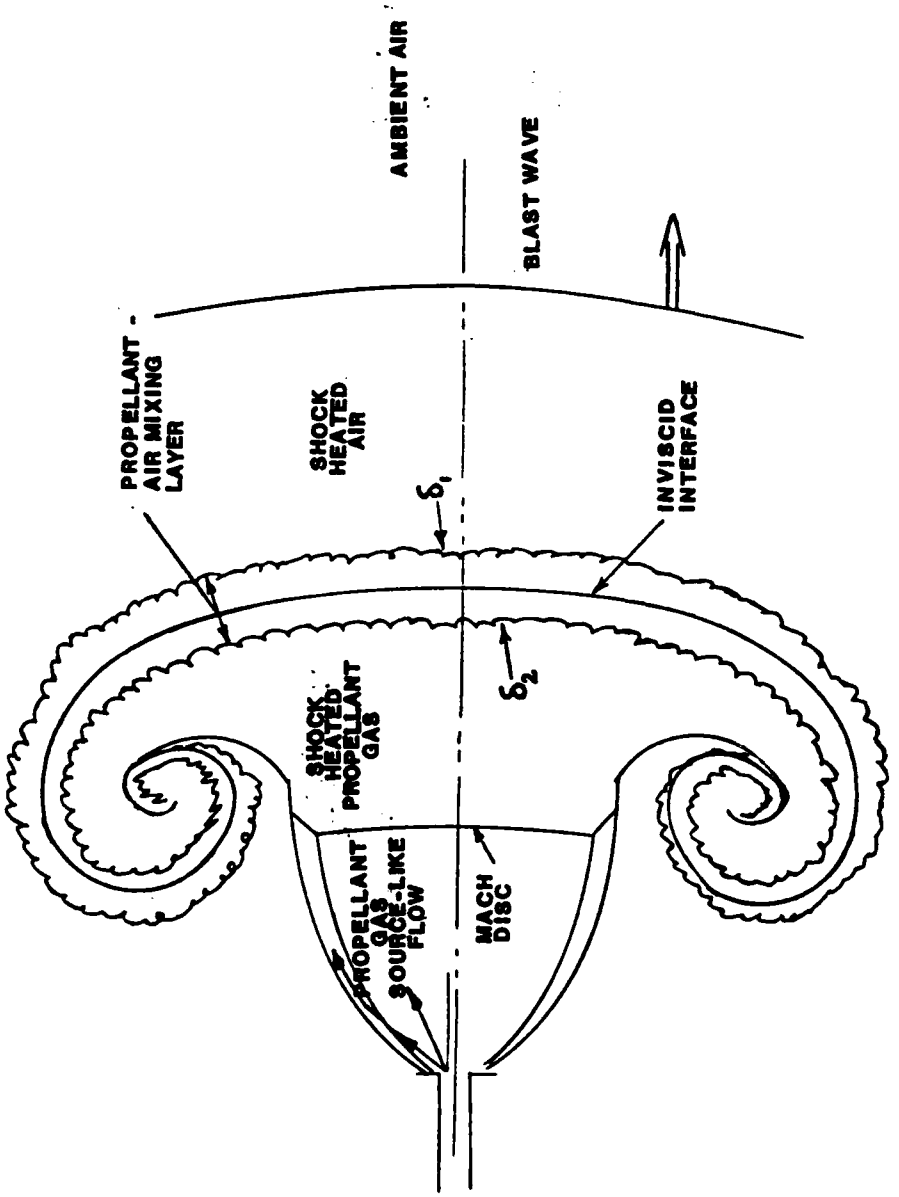

FIGURE 1. SCHEMATIC OF MUZZLE BLAST FLOWFIELD

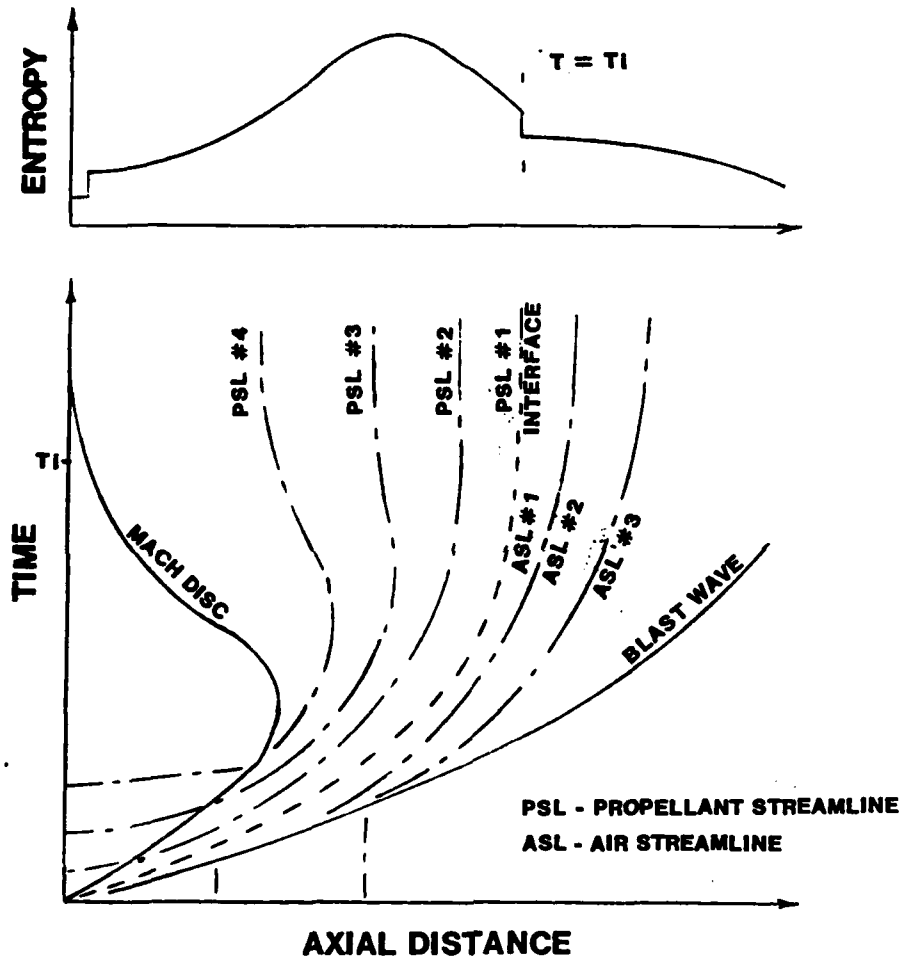

FIGURE 2. SCHEMATIC SHOWING TYPICAL STREAMLINE TRACES AND ENTROPY DISTRIBUTION

```
1.E-5      1.0E-3     0.5
.00052     .0200      0.1          .5085      2.704E+01 1.020E+08
    0 9000    01    -0     1     0
   11     5
 .0000E+00 .2955E+00   28.0150          CO
 .0000E+00 .1785E+00   44.0099          CO2
 .0000E-05 .2939E-05    1.0080          H
 .0000E-01 .1257E-01    2.0159          H2
 .0000E+00 .1711E+00   18.0153          H2O
 .7655E+00 .3268E+00   28.0134          N2
 .0000E-08 .9712E-08   15.9994          O
 .0000E-05 .6403E-05   17.0074          OH
 .2345E-00 .1355E-08   31.9988          O2
 .0000E-02 .1450E-02   39.1000          K
 .0000E-01 .1408E-01   56.0100          KOH
```

FIGURE 3. TYPICAL INPUT DATA FILE FOR UMLAC (LOGICAL UNIT 5)

```
 11    11    0   11   15    21    29    35    40    45    69    73    76
            CO          CO2            H            H2           H2O           N2     ] LINES 2 AND 3
             O           OH           O2             K           KOH                  ] ARE NOT USED
.800028E+00 .139342E+02 .412693E+01 .392245E+01 .000000E+00 .000000E+00
.000000E+00 .000000E+00 .000000E+00 .000000E+00 .000000E+00 .000000E+00
.000000E+00 .000000E+00
.300099E+00 .177102E+00 .157026E-07 .128998E-01 .171237E+00 .332200E+00  ] PROPELLENT
.200229E-10 .133107E-08 .688885E-08 .500073E-03 .603633E-02              ] SIDE
.280150E-18 .440099E-18 .100800E-19 .201590E-19 .180153E-18 .765000E+00 ] AIR
.360004E-18 .170074E-18 .235000E+00 .391000E-18 .560100E-18             ] SIDE
.300100E+00 .177100E+00 .181000E-05 .129000E-01 .171200E+00 .332200E+00  ] 2nd
.515900E-08 .373200E-05 .688900E-08 .426300E-03 .614200E-02              ] STREAMLINE
.300100E+00 .177100E+00 .181000E-05 .129000E-01 .171200E+00 .332200E+00
.515900E-08 .373200E-05 .688900E-08 .426300E-03 .614200E-02
.300100E+00 .177100E+00 .181000E-05 .129000E-01 .171200E+00 .332200E+00
.515900E-08 .373200E-05 .688900E-08 .426300E-03 .614200E-02
.300100E+00 .177100E+00 .181000E-05 .129000E-01 .171200E+00 .332200E+00
.515900E-08 .373200E-05 .688900E-08 .426300E-03 .614200E-02
.300100E+00 .177100E+00 .181000E-05 .129000E-01 .171200E+00 .332200E+00
.515900E-08 .373200E-05 .688900E-08 .426300E-03 .614200E-02
.300100E+00 .177100E+00 .181000E-05 .129000E-01 .171200E+00 .332200E+00
.515900E-08 .373200E-05 .688900E-08 .426300E-03 .614200E-02
.300100E+00 .177100E+00 .181000E-05 .129000E-01 .171200E+00 .332200E+00
.515900E-08 .373200E-05 .688900E-08 .426300E-03 .614200E-02
.300100E+00 .177100E+00 .181000E-05 .129000E-01 .171200E+00 .332200E+00
.515900E-08 .373200E-05 .688900E-08 .426300E-03 .614200E-02
.300100E+00 .177100E+00 .181000E-05 .129000E-01 .171200E+00 .332200E+00
.515900E-08 .373200E-05 .688900E-08 .426300E-03 .614200E-02
.300100E+00 .177100E+00 .181000E-05 .129000E-01 .171200E+00 .332200E+00
.515900E-08 .373200E-05 .688900E-08 .426300E-03 .614200E-02
.282910E+01 .282910E+01 .000000E+00 .000000E+00 .000000E+00 .000000E+00   END OF FIRST
.000000E+00 .000000E+00 .000000E+00 .000000E+00 .000000E+00 .000000E+00   DATA SET
------------------------------------------------------------------------------------
.877322E+00 .170213E+02 .476306E+01 .461163E+01 .000000E+00 .000000E+00   START OF SECOND
.000000E+00 .000000E+00 .000000E+00 .000000E+00 .000000E+00 .000000E+00   DATA SET
.000000E+00 .000000E+00
......
```

FIGURE 4. TYPICAL BOUNDARY CONDITION DATA FILE FOR UMLAC (LOGICAL UNIT 9)

```
ELEMENTS
C         12.01115  4.000000
H          1.007970 1.000000
O         15.999400-2.000000
N         14.006700 3.0
K         39.100000 1.0

THERMO
CO                J 9/65C  1.0  1.00 0.00 0.G   300.000  5000.000
 0.29840689E 01 0.14891387E-02-0.57899678E-06 0.10364576E-09-0.69353499E-14
-0.14245227E 05 0.63479147E 01 0.37100916E 01-0.16190964E-02 0.36923584E-05
-0.20319673E-08 0.23953344E-12-0.14356309E 05 0.29555340E 01
CO2               J 9/65C  1.0  2.00 0.00 0.G   300.000  5000.000
 0.44608040E 01 0.30981717E-02-0.12392566E-05 0.22741323E-09-0.15525948E-13
-0.48961438E 05-0.98635978E 00 0.24007788E 01 0.87350905E-02-0.66070861E-05
 0.20021860E-08 0.63274039E-15-0.48377520E 05 0.96951447E 01
H                 J 9/65H  1.00 0.00 0.00 0.G   300.000  5000.000
 0.25000000E 01 0.0            0.0            0.0            0.0
 0.25471625E 05-0.46011758E 00 0.25000000E 01 0.0            0.0
 0.0            0.0            0.25471625E 05-0.46011758E 00
H2                J 3/61H  2.0  0.0  0.0  0.G   300.000  5000.000
 0.31001883E 01 0.51119458E-03 0.52644204E-07-0.34909964E-10 0.36945341E-14
-0.87738013E 03-0.19629412E 01 0.30574446E 01 0.26765198E-02-0.58099149E-05
 0.55210343E-08-0.18122726E-11-0.98890430E 03-0.22997046E 01
H2O               J 3/61H  2.0  1.00 0.00 0.G   300.000  5000.000
 0.27167616E 01 0.29451370E-02-0.80224368E-06 0.10226681E-09-0.48472104E-14
-0.29905820E 05 0.66305666E 01 0.40701275E 01-0.11084499E-02 0.41521180E-05
-0.29637404E-08 0.80702101E-12-0.30279719E 05-0.32270038E 00
N2                J 9/65N  2.0  0.0  0.0  0.G   300.000  5000.000
 0.28963194E 01 0.15154863E-02-0.57235275E-06 0.99807385E-10-0.65223536E-14
-0.90586182E 03 0.61615143E 01 0.36748257E 01-0.12081496E-02 0.23240100E-05
-0.63217520E-09-0.22577253E-12-0.10611587E 04 0.23580418E 01
O                 J 6/62O  1.00 0.00 0.00 0.G   300.000  5000.000
 0.25420580E 01-0.27550603E-04-0.31028029E-08 0.45510670E-11-0.43680494E-15
 0.29230801E 05 0.49203072E 01 0.29464283E 01-0.16381664E-02 0.24210303E-05
-0.16028432E-08 0.38906964E-12 0.29147641E 05 0.29639931E 01
OH                J 3/66O  1.H  1.00 0.00 0.G   300.000  5000.000
 0.29106417E 01 0.95931627E-03-0.19441700E-06 0.13756646E-10 0.14224542E-15
 0.39353811E 04 0.54423428E 01 0.38375931E 01-0.10778855E-02 0.96830354E-06
 0.18713971E-09-0.22571089E-12 0.3( 412820E 04 0.49370009E 00
O2                J 9/65O  2.0  0.0  0.0  0.G   300.000  5000.000
 0.36219521E 01 0.73618256E-03-0.19652219E-06 0.36201556E-10-0.28945623E-14
-0.12019822E 04 0.36150942E 01 0.36255980E 01-0.18782183E-02 0.70554543E-05
-0.67635071E-08 0.21555977E-11-0.10475225E 04 0.43052769E 01
K                 J     K  1.   0.0  0.0  0.G   300.000  5000.000
 0.2561E     01-0.1373E    -03 .1160E     -06-0.5159E    -10 0.1180E    -13
 -0.7658E    03 0.4699E     01 0.2403E    +01 0.6656E    -03-0.1599E    -05
 0.1615E    -08-.5843E     -12-0.7349E     03 0.5440E     01
KOH               J     K  1.0  1.H  1.   0.G   300.000  5000.000
 0.5643E     01  0.1243E   -02-0.3424E    -06 0.4206E    -10-0.1816E    -14
 -0.4035E    05 -0.4072E    01 0.3663E     01 0.1268E    -01-0.2348E    -04
 0.2008E    -07-0.6357E    -11-0.4011E     05 0.4643E     01

MECHANISM -YOSEFIAN RATE CONSTANTS FOR MUZZLE BLAST
CO      OH              CO2     H               4.227   1.3     -330.
CO      O2              CO2     O               9.403   0.0     24000.
CO      O       M       CO2             M       9.4046  0.0     2200.
H       O2              OH      O               11.16   0.0     8250.
O       H2              OH      H               7.2569  1.0     4480.
OH      OH              H2O     O               9.780   0.0     550.
OH      H2              H       H2O             6.06    1.3     1825.
O       H       M       OH              M       12.559  -1.     0.0
O       O       M       O2              M       8.0366  0.0     -900.
H       OH      M       H2O             M       16.559  -2.     0.0
H       H       M       H2              M       12.0366 -1.0    0.0
H       KOH             H2O     K               10.035  0.0     1000.
K       OH      M       KOH             M       14.7353 -1.     0.0
```

FIGURE 5. TYPICAL THERMODYNAMIC AND REACTION KINETICS DATA FILE FOR UMLAC AND CREK (LOGICAL UNIT 15)

```
          UNSTEADY MIXING LAYER MODEL
```

OUTPUT HEADER

```
          INPUT DATA:

  .1000E-04 .1000E-02 .5000E+00
  .5200E-03 .2000E-01 .1000E+00 .5085E+00 .2704E+02 .1020E+09
     0 9000    1    0    1    0
    11    5
   .295E+00  .295E+00  .280E+02          CO
   .178E+00  .178E+00  .440E+02          CO2
   .294E-05  .294E-05  .101E+01          H
   .126E-01  .126E-01  .202E+01          H2
   .171E+00  .171E+00  .180E+02          H2O
   .327E+00  .327E+00  .280E+02          N2
   .971E-08  .971E-08  .160E+02          O
   .640E-05  .640E-05  .170E+02          OH
   .135E-08  .135E-08  .320E+02          O2
   .145E-02  .145E-02  .391E+02          K
   .141E-01  .141E-01  .560E+02          KOH
```

INPUT DATA (CARD IMAGE FORMAT) FROM LU #5

```
 DINF,CPINF,PINF,RHOINF,CINF,TINF,MWINF,TMINF
  .5085E+00   .6006E+04   .2117E+04   .2376E-02   .9439E+03   .5192E+03   .2889E+02   .5387E-03
```

SCALE FACTORS USED FOR NONDIMENSIONALIZATION

FIGURE 6. TYPICAL OUTPUT DATA FROM UMLAC (LOGICAL UNIT 6)

```
 92 ENTRIES HAVE BEEN READ FROM TAPE 9.

STREAMLINE  1 STARTS AT T =   .4310E-03 SEC. WITH Y =   .1439E+01 FT.
STREAMLINE  2 STARTS AT T =   .1079E-02 SEC. WITH Y =   .3282E+01 FT.
STREAMLINE  3 STARTS AT T =   .1435E-02 SEC. WITH Y =   .4020E+01 FT.
STREAMLINE  4 STARTS AT T =   .2026E-02 SEC. WITH Y =   .4971E+01 FT.
STREAMLINE  5 STARTS AT T =   .2899E-02 SEC. WITH Y =   .5811E+01 FT.
STREAMLINE  6 STARTS AT T =   .3603E-02 SEC. WITH Y =   .6175E+01 FT.
STREAMLINE  7 STARTS AT T =   .4246E-02 SEC. WITH Y =   .6478E+01 FT.
STREAMLINE  8 STARTS AT T =   .5057E-02 SEC. WITH Y =   .6637E+01 FT.
STREAMLINE  9 STARTS AT T =   .1321E-01 SEC. WITH Y =   .5486E+01 FT.
STREAMLINE 10 STARTS AT T =   .1551E-01 SEC. WITH Y =   .5254E+01 FT.
STREAMLINE 11 STARTS AT T =   .1742E-01 SEC. WITH Y =   .4605E+01 FT.
```

SYNOPSIS OF STREAMLINE DATA FROM LU #9

```
WARNING...THE BOUNDARY CONDITION DATA ENDS AT T =   .2898E-01 SEC.  THE PROGRAM WILL NOT EXTRAPOLATE THE BOUNDARY DATA.
```


AIR SIDE $y = \delta_1$	PROPELLENT SIDE, $y = \delta_2$		
.280E-18	.300E+00	.280E+02	CO
.440E-18	.177E+00	.440E+02	CO2
.101E-19	.157E-07	.101E+01	H
.202E-19	.129E-01	.202E+01	H2
.180E-18	.171E+00	.180E+02	H2O
.765E+00	.332E+00	.280E+02	N2
.360E-18	.200E-10	.160E+02	O
.170E-18	.133E-08	.170E+02	OH
.235E+00	.689E-08	.320E+02	O2
.391E-18	.500E-03	.391E+02	K
.560E-18	.604E-02	.560E+02	KOH

CALCULATED INITIAL CONDITIONS FOR THE SPECIES

1

FIGURE 6. (Continued)

```
      K      TIME          DELTA1        DELTA2        THETA**2        PHI           RHO          KTO
      0    .52000E-03    .10000E-01   -.10000E-01    .27040E+02    .10200E+09    .51721E+01
        4       1       1    1.85629E-02

1

      K      TIME          DELTA1        DELTA2        THETA**2        PHI           RHO          KTO
      1    .53000E-03    .10057E-01   -.10055E-01    .27040E+02    .10200E+09    .51559E+01    .57179E-04

             P            RH1           RH2          TEMP1         TEMP2         YZERO
         .19400E+02    .51200E+01    .51961E+01    .19652E+04    .15744E+04   -.18420E+01

 TEMP,H,ALPHA  .175034E+04 -.183932E+08
  .150050E+00  .885511E-01  .120034E-09  .644990E-02  .856185E-01  .548600E+00  .234473E-09  .635315E-10
.117500E+00  .250360E-03  .301770E-02

 DPDT,DRH1DT,DRH2DT: -.435917E+01 -.922514E+00 -.882831E+00

 ALPHA1:  .280151E-18  .440101E-18  .100800E-19  .201591E-19  .180154E-18  .765000E+00  .265254E-16  .623912E-1
.235000E+00  .391002E-18  .560103E-1

 DALP1DT:  .000000E+00  .000000E+00  .000000E+00  .000000E+00  .000000E+00  .000000E+00  .192425E-15  .273224E-07
.000000E+00  .000000E+00  .000000E+

 ALPHA2:  .300099E+00  .177102E+00  .615547E-08  .128998E-01  .171237E+00  .332200E+00  .262902E-10  .539262E-09
.688886E-08  .500254E-03  .603606E-0

 DALP2DT:  .000000E+00  .000000E+00 -.524727E-08  .000000E+00  .000000E+00  .000000E+00 -.222821E-10 -.458337E-09
.000000E+00  .202235E-06 -.291871E-
       4       1       1    1.85629E-02
       1
    1.16018E-03
    1.16018E-03

1
```

OUTPUT AT K = 0

OUTPUT AT K = 1

FIGURE 6. (Cont.)

```
     K      TIME          DELTA1        DELTA2        THETA**2        PHI           RHO          KTO
    10    .53531E-03    .10087E-01  -.10084E-01    .27040E+02    .10200E+09    .51472E+01    .59189E-04

           P           RH1           RH2          TEMP1         TEMP2         YZERO
         .19286E+02    .50959E+01    .51749E+01    .19629E+04    .15716E+04  -.18635E+01

 TEMP,H,ALPHA   .174301E+04 -.184522E+08
  .150050E+00   .885511E-01   .134496E-09   .644990E-02   .856185E-01   .548600E+00   .263683E-09   .709277E-10
.117500E+00   .250374E-03   .301769E-02

 DPDT,DRH1DT,DRH2DT: -.435917E+01 -.922514E+00 -.881632E+00

 ALPHA1:   .280151E-18   .440101E-18   .100800E-19   .201591E-19   .180154E-18   .765000E+00   .284230E-16   .650855E-18
.235000E+00   .391002E-18   .560103E-1

 DALP1DT:   .000000E+00   .000000E+00   .000000E+00   .000000E+00   .000000E+00   .000000E+00   .192425E-15   .273224E-17
.000000E+00   .000000E+00   .000000E+

 ALPHA2:   .300099E+00   .177102E+00   .596018E-08   .128998E-01   .171237E+00   .332200E+00   .254560E-10   .522141E-09
.688886E-08   .500266E-03   .603604E-0

 DALP2DT:   .000000E+00   .000000E+00 -.512451E-08   .000000E+00   .000000E+00   .000000E+00 -.217570E-10 -.447545E-09
.000000E+00   .197468E-06 -.284991E-
       4       1       1   2.32041E-03
       1
    4.64073E-03
    4.64073E-03
1
```

OUTPUT AT K = 10

FIGURE 6. (Concluded)

DISTRIBUTION LIST

No. of Copies	Organization
12	Administrator Defense Technical Info Center ATTN: DTIC-FDAC Cameron Station, Bldg. 5 Alexandria, VA 22304-6145
1	Commander US Army Materiel Command ATTN: AMCDRA-ST 5001 Eisenhower Avenue Alexandria, VA 22333-0001
1	Commander US Army Materiel Command ATTN: AMCLDC 5001 Eisenhower Avenue Alexandria, VA 22333
1	Commander US Army Laboratory Command ATTN: AMSLC-TD, Richard Vitali 2800 Powder Mill Road Adelphi, MD 20783-1145
1	Commander US Army Materiel Command ATTN: AMCDRA-ST, R. Haley 5001 Eisenhower Avenue Alexandria, VA 22333-0001
1	HQDA DAMA-ART-M Washington, DC 20310
1	HQDA ATTN: DAMA-ARZ-A, COL. J. Kempster Pentagon, Room 3-E-426 Washington, DC 20310-0632
1	HQDA ATTN: DAMA-ARZ-A, COL. N. Cooney Pentagon, Room 3-E-426 Washington, DC 20310-0632

Copies	Organization
1	Commander US Army Aviation Systems Command ATTN: AMSAV-ES 4300 Goodfellow Boulevard St. Louis, MO 63120-1798
1	Director US Army Aviation Research and Technology Activity Ames Research Center Moffett Field, CA 94035-1099
1	Commander CECOM R&D Technical Library ATTN: AMSEL-IM-L (Reports Section) Bldg. 2700 Fort Monmouth, NJ 07703-5000
1	President US Army Aviation Test Board ATTN: ATZQ-OP-AA Ft. Rucker, AL 36360
1	Commander US Army Communications - Electronics Command ATTN: AMSEL-ED Fort Monmouth, NJ 07703-5016
1	Commander US Army Research Development & Engineering Center ATTN: AMSMI-RD Redstone Arsenal, AL 35898
1	Commander US Army Missile Command ATTN: AMSMI-RBL Redstone Arsenal, AL 35898
1	Commander US Army Missile Command ATTN: AMSMI-TLH Redstone Arsenal, AL 35898

DISTRIBUTION LIST

No. of Copies	Organization
1	Commander US Army Missile Command ATTN: AMSMI-RDK Redstone Arsenal, AL 35898-5249
1	Director US Army Missile & Space Intelligence Center ATTN: AIAMS-YDL Redstone Arsenal, AL 35898-5500
1	Commander US Army Tank Automotive Command ATTN: AMSTA-TSL Warren, MI 48397-5000
1	Commander US Army Operational Test and Evaluation Agency ATTN: CSTE-ZS 5600 Columbia Pike Falls Church, VA 22041
1	Commander US Army Armament Munitions & Chemical Command ATTN: AMSMC-IMP-L Rock Island, IL 61299-7300
10	Commander US Army ARDEC ATTN: SMCAR-MSI SMCAR-TDC SMCAR-TDS, Mr. Lindner SMCAR-LC-F, Mr. Loeb SMCAR-LCW, Mr. Salsbury SMCAR-LCW, Mr. R. Wrenn SMCAR-SCA, Mr. Gehbauer SMCAR-LCU, Mr. Barrieres SMCAR-LC, T. Davidson Dover, NJ 07801-5001
1	Project Manager Tank Maintenance Armament Systems ATTN: PM 105 Systems Dover, NJ 07801-5001
1	Project Manager Tank Maintenance Armament Systems ATTN: AMCPM-TM-A, Harvey Yuen H. Kosser W. Lang Dover, NJ 07801-5001
1	Commander US Army Development and Employment Agency ATTN: MODE-TED-SAB Fort Lewis, WA 98433
1	Commander Armament RD&E Center US Army AMCCOM ATTN: SMCAR-TDC Dover, NJ 07801
1	LT COL Alexander Lancaster Tactical Technology Office Defense Advanced Research Projects Agency 1400 Wilson Boulevard Arlington, VA 22209
1	ODCSI, USAREUR / 7A ATTN: AEAGB-PDN(S&E) APO, NY 09403
4	Commander US AMCCOM ARDEC CCAC Benet Weapons Laboratory ATTN: SMCAR-LCB-TL Dr. T. Simkins Dr. G. Carofano Dr. C. Andrade Watervliet, NY 12189-4050
1	Commander US Army Materials Technology Laboratory ATTN: SLCMR-ATL Watertown, MA 02172

DISTRIBUTION LIST

No. of Copies	Organization
1	Commander US Army Natick Research and Development Laboratory ATTN: AMDNA, Dr. D. Sieling Natick, MA 01760
1	Director US Army TRADOC Analysis Center ATTN: ATOR-TSL White Sands Missile Range, NM 88002-5502
1	Commandant US Army Infantry School ATTN: ATSH-CD-CS-OR Ft. Benning, GA 31905-5400
1	Commander US Army Development and Employment Agency ATTN: MODE-ORO Fort Lewis, WA 98433-5000
1	Commander US Army Research Office ATTN: CRD-AA-EH P.O. Box 12211 Research Triangle Park, NC 27709-2211
1	President US Army Armor and Engineer Board ATTN: ATZK-AE-PD, Mr. W. Wells Ft. Knox, KY 40121
1	Commander Naval Air Systems Command ATTN: AIR-604 Washington, DC 20360
1	Commander Naval Sea Systems Cmd ATTN: 003 Washington, DC 20362
1	Commander Naval Weapons Center ATTN: Dr. Klaus Schadow Code 3892 China Lake, CA 93555
2	Commander David W. Taylor Naval Ship Research & Development Ctr ATTN: Lib Div, Code 522 Aerodynamic Lab Bethesda, MD 20084
2	Commander Naval Surface Weapons Center ATTN: 6X Dr. J. Yagla Dr. G. Moore Dahlgren, VA 22448
1	Commander Naval Surface Weapons Center ATTN: Code 730 Silver Spring, MD 20910
1	Commander Naval Weapons Center ATTN: Code 3433, Tech Lib China Lake, CA 93555
1	Commander Naval Ordnance Station ATTN: Code FS13A, P. Sewell Indian Head, MD 20640
1	AFWL/SUL Kirtland AFB, NM 87117
1	AFATL/DOIL (Tech Info Center) Eglin AFB, FL 32542-5000
1	ASD/XRA (Stinfo) Wright-Patterson AFB, OH 45433

DISTRIBUTION LIST

No. of Copies	Organization
1	Director National Aeronautics and Space Administration George C. Marshall Space Flight Center ATTN: MS-I, Lib Huntsville, AL 38512
1	NASA Langley Research Center ATTN: G. B. Northam Mail Stop 168 Hampton, VA 23665
1	Director Jet Propulsion Laboratory ATTN: Tech Lib 4800 Oak Grove Drive Pasadena, CA 91109
1	Director NASA Scientific & Technical Information Facility ATTN: SAK/DL P.O. Box 8757 Baltimore/Washington International Airport, MD 21240
1	AAI Corporation ATTN: Dr. T. Stastny P.O. Box 126 Cockeysville, MD 21030
1	Advanced Technology Labs ATTN: Mr. J. Erdos Merrick & Steward Avenues Westbury, NY 11590
2	United Technologies/Chemical Systems ATTN: Dr. Richard MacLaren Mr. Allen Holzman P.O. Box 50015 San Jose, CA 95150-0015
1	Science Applications, International Corporation ATTN: Dr. Raymond Edleman 9760 Gwensmouth Avenue Chatworth, CA 91311
1	Aerospace Corporation ATTN: Dr. G. Widhopf Bldg. D8 M4/965 P.O. Box 92957 Los Angeles, CA 90009
1	AVCO Systems Division ATTN: Dr. D. Siegelman 201 Lowell Street Wilmington, MA 01887
1	Technical Director Colt Firearms Corporation 150 Huyshope Avenue Hartford, CT 14061
1	General Electric Armament & Electric Systems ATTN: Mr. R. Whyte Lakeside Avenue Burlington, VT 05401
2	Honeywell, Inc. ATTN: Mail Station MN 112190, G. Stilley MN 50-2060, Mr. T. Melander 600 Second Street, North East Hopkins, MN 55343
1	Hughes Helicopter Company Bldg. 2, MST22B ATTN: Mr. R. Forker Centinela and Teale Streets Culver City, CA 90230
1	Martin Marietta Aerospace ATTN: Mr. A. J. Culotta P.O. Box 5837 Orlando, FL 32805
1	AEROJET Ordnance Company ATTN: Mr. A. Flatau 2521 Michelle Drive Tustin, CA 92680

DISTRIBUTION LIST

No. of Copies	Organization
1	S.K. Martini, Tech Reports Center Olin Corp. Research Center 350 Knotter Drive Cheshire, CT 06410-0586
1	Director Sandia National Laboratory ATTN: Aerodynamics Dept Org 5620, R. Maydew Albuquerque, NM 87115
1	Guggenheim Aeronautical Lab California Institute of Tech ATTN: Tech Lib Pasadena, CA 91104
1	Franklin Institute ATTN: Tech Lib Race & 20th Streets Philadelphia, PA 19103
1	Director Applied Physics Laboratory The Johns Hopkins University Johns Hopkins Road Laurel, MD 20707
1	Massachusetts Institute of Technology Dept of Aeronautics and Astronautics ATTN: Tech Lib 77 Massachusetts Avenue Cambridge, MA 02139
1	Ohio State University Dept of Aeronautics and Astronautical Engineering ATTN: Tech Lib Columbus, OH 43210
1	Arizona State University ATTN: Dr. R. M. C. So Tempe, Arizona 85281
1	Polytechnic Institute of New York Graduate Center ATTN: Tech Lib Route 110 Farmingdale, NY 11735
2	Loral Corporation ATTN: S. Schmotolocha Ben Axley 300 N. Halstead St. P.O. Box 7101 Pasadena, CA 91109
1	Director Forrestal Research Center Princeton University Princeton, NJ 08540
1	Kaman Tempo ATTN: Mr. J. Hindes 816 State Street P.O. Drawer QQ Santa Barbara, CA 93102
1	Southwest Research Institute ATTN: Mr. Peter S. Westine P.O. Drawer 28510 8500 Culebra Road San Antonio, TX 78228
1	Boeing Corporation ATTN: C. R. Pond MS 8C-64 PO Box 3999 Seattle, WA 98124
1	General Defense Corporation Flinchbaugh Division ATTN: Mr. Edwin Steiner 200 East High Street P.O. Box 127 Red Lion, PA 17356
1	FMC Corporation Northern Ordnance Division ATTN: Scott Langlie, Advanced Techniques 4800 East River Road Minneapolis MN 55421

DISTRIBUTION LIST

No. of Copies	Organization
10	C.I.A. OIR/DB/Standard GE-47 HQ Washington, D.C. 20505

Aberdeen Proving Ground

Dir, USAMSAA
ATTN: AMXSY-D
AMXSY-MP, H. Cohen

Cdr, USATECOM
ATTN: AMSTE-SI-F

Cdr, CRDC, AMCCOM
ATTN: SMCCR-RSP-A
SMCCR-MU
SMCCR-SPS-IL

Dir, USAHEL
ATTN: Dr. Weisz
Dr. Cummings
Mr. Garinther

Dir, USACSTA
ATTN: Mr. S. Walton

USER EVALUATION SHEET/CHANGE OF ADDRESS

This Laboratory undertakes a continuing effort to improve the quality of the reports it publishes. Your comments/answers to the items/questions below will aid us in our efforts.

1. BRL Report Number _____ Date of Report _____

2. Date Report Received _____

3. Does this report satisfy a need? (Comment on purpose, related project, or other area of interest for which the report will be used.) _____

_____

_____

4. How specifically, is the report being used? (Information source, design data, procedure, source of ideas, etc.) _____

_____

_____

5. Has the information in this report led to any quantitative savings as far as man-hours or dollars saved, operating costs avoided or efficiencies achieved, etc? If so, please elaborate. _____

_____

_____

6. General Comments. What do you think should be changed to improve future reports? (Indicate changes to organization, technical content, format, etc.)

_____

_____

_____

CURRENT ADDRESS

_____
Name

_____
Organization

_____
Address

_____
City, State, Zip

7. If indicating a Change of Address or Address Correction, please provide the New or Correct Address in Block 6 above and the Old or Incorrect address below.

OLD ADDRESS

_____
Name

_____
Organization

_____
Address

_____
City, State, Zip

(Remove this sheet along the perforation, fold as indicated, staple or tape closed, and mail.)

FOLD HERE

Director
U.S. Army Ballistic Research Laboratory
ATTN: SLCBR-DD-T
Aberdeen Proving Ground, MD 21005-5066

NO POSTAGE
NECESSARY
IF MAILED
IN THE
UNITED STATES

OFFICIAL BUSINESS
PENALTY FOR PRIVATE USE, $300

BUSINESS REPLY MAIL
FIRST CLASS PERMIT NO 12062 WASHINGTON, DC
POSTAGE WILL BE PAID BY DEPARTMENT OF THE ARMY

Director
U.S. Army Ballistic Research Laboratory
ATTN: SLCBR-DD-T
Aberdeen Proving Ground, MD 21005-9989

FOLD HERE